الجمهورية الجزائرية الديمقراطية الشعبية
DEMOCRATIC AND POPULAR ALGERIAN REPUBLIC
MINISTRY OF HIGHER EDUCATION
AND SCIENTIFIC RESEARCH



MOHAMED SEDDIK BENYAHIA JIJEL UNIVERSITY
Faculty of science and technology
Mechanical Engineering Department

N°:……/2025

Graduation Thesis

DOMAINE: Science and Technology

FIELD: Mechanical Engineering

SPECIALITY: Energy

Theme

Optimization of a PVT solar collector performance by reducing the flow passage section

Presented by:
MAPFUMO Redeemer

Supervised by:
Dr. BOUROUIS Abderahim

Date of Graduation: 02/07/2025

Graduation Jury

President: Ghellab A.	Grade MCA	Univ MSB Jijel
Supervisor: Bourouis A.	Grade MCA	Univ MSB Jijel
Examiner: Bouraoui A.	Grade MCB	Univ MSB Jijel

Promotion 2024/2025

Acknowledgements

First and foremost, I am sincerely grateful to God for granting me the health, strength and determination to complete this modest work.

My deepest gratitude goes to Professor A Bourouis, my supervisor, whose invaluable guidance, support, and insightful feedback were instrumental in the successful completion of this thesis. His expertise and patience significantly shaped the research's direction and quality.

I also express sincere thanks to the University of Jijel, specifically the Faculty of Science and Technology and the Department of Mechanical Engineering, for providing a stimulating environment and the necessary resources throughout my academic journey. The department's commitment to excellence inspired my research.

I am particularly grateful to Madam Sonya, the international student representative, for her support and creating a welcoming atmosphere.

My appreciation extends to my classmates, whose collaboration on assignments and practical work was invaluable.

Finally, I acknowledge the many others who indirectly contributed to this research. This work would not have been possible without the collective support and contributions of all mentioned, and I am profoundly thankful for their assistance and encouragement.

Dedication

I dedicate this modest research to my family and friends, whose unwavering support and understanding were invaluable throughout my academic journey. Their love, encouragement, and belief in my abilities provided constant motivation.

To my dear parents, my gratitude is beyond measure. Your love, kindness, and unwavering presence have been my strength, enabling me to overcome every challenge. Your faith in me empowers me to reach new heights, even when self-doubt arises.

To my brothers and sisters, this work is offered as a testament to your limitless potential, encouraging you to pursue your aspirations with unwavering determination. I love you all.

Finally, to my family in Jijel, fellow international students, I cherish the bond we share and I wish you continued success in your studies.

Summary

List of figures……III

List of tables……...V

Nomenclature……VI

General Introduction……2

Chapter I

I.1. Introduction……5
I.2. Renewable Energies……5
1.2.1. Forms of renewable energies……..6
I.3. Solar Collectors……..…7
I.3.1. Photovoltaic Solar Collectors……..8
I.3.1.1. The photovoltaic effect……8
I.3.1.2. An off grid Photovoltaic solar system……..…8
I.3.1.3. Principal components of solar PV modules……..9
I.3.1.4. Interconnection between PV Modules……...….10
I.3.1.5. Working Principle of a PV Cell……..11
I.3.1.6. Types of PV cells……12
I.3.1.7. Effect of Temperature on PV Solar cells……13
I.3.2. Thermal solar collectors……14
I.3.2.1. Commercial thermal solar collectors……..14
I.3.2.2. Domestic thermal solar collectors……..15
I.3.3. Photovoltaic Thermal Solar Collectors……15
I.3.3.1. Description ……15
I.3.3.2. Different Types of PVT modules……...16
I.3.4. Bibliographic Research on PVT Systems……18
I.3.4.1. History of PVT systems……18

Chapter II

II.1. Introduction……30
II.2. Geometry and Mathematical Model……30

II.2.1. Specifications of the studied PVT collectors……...31
II.2.2. Simplification Assumptions…….31
II.2.3. Mathematical Formulations…….32
II.3. Efficiencies of the PVT system……..……33
II.3.1. Thermal Efficiency……..34
II.3.2. Electrical Efficiency……34
II.3.3. Overall Efficiency……...35
II.4. Numerical processing and mesh effect……...35
II.4.1. The simple algorithm……...35
II.4.2. Convergence criteria (residual)……...….35
II.4.3. The mesh effect……37
II.4.4. Code validation……37

Chapter III

III.1. Introduction……40
III.2. Case 1: Classical PVT collector…….40
III.3. Case 2: Effect of solid layer insertion……45
III.3.1. Effect of Solid layer height…….45
III.3.2. Effect of solid layer length……..48
General conclusion……52
References…….54

List of Figures

Chapter I

Figure I.1. Different sources of renewable energies……7
Figure I.2. An off grid photovoltaic solar system……..8
Figure I.3. The main components of a PV module……9
Figure I.4. Series, parallel and mixed configuration of solar PV modules……11
Figure I.5. Common PV module technologies……12
Figure I.6. Effect of temperature on the Power output of PV cell……13
Figure I.7. Parabolic solar collectors……14
Figure I.8. Domestic thermal solar collectors……...15
Figure I.9. Possible configurations in air-based PVT modules……17
Figure I.10. Possible configurations in water-based PV/T modules……18
Figure I.11. Design of the solar photovoltaic/thermal (PVT) air/water heating system……..19
Figure I.12 Configurations of the single-pass and the double pass PVT collectors……20
Figure I.13. The structure of the building incorporated with hybrid wallboard……21
Figure I.14. Cross-sectional view of PVT/AIR collector models. Fluid flow is perpendicular to the page……..22
Figure I.15. Solar Photovoltaic thermal air collector equipped with tunnels……22
Figure I.16. PVT collector with stainless-steel wool, honeycomb and V-groove heat exchangers……23
Figure I.17. Schematic cross-sectional view of: photovoltaic module (PV-I), basic solar PVT air collector (PVT-II), glazed solar PVT air collector (PVT-III) and glazed double-pass solar PVT air collector (PVT-IV)……..24
Figure I.18 Schematic diagram of the nanofluid PVT system……25
Figure. I.19 Configuration of the PVT-PCM module showing heat transfer modes……26
Figure I.20 Schematic diagram of the PVT integrated with a porous medium……27

Chapter 2

Figure II.1. Schematic of the studied PVT collector.
(a) Schematic of the traditional PVT collector……...30
(b) Schematic of the modified PVT collector……31

Figure II.2 Representative diagram of the SIMPLE algorithm…….36

Figure II.3. Meshing effect on the average outlet and average PV cells temperatures……37

Figure II.4. Validation of code

(a) Validation of the U-velocity profiles with those of Hooman, as a function of S…….38

(b) Validation of Nusselt number with the one of Radwan et al. for different heating positions……38

Chapter 3

Figure III.1. Solar radiation levels throughout the day in summer, winter, and spring……..41

Figure III.2 (a) velocity contours and (b) thermal fields for different values of Reynolds number (Re = 500 to 2000) and solar radiation (ϕ = 1000W/m^2).

(a) Velocity contours……41

(b) Isotherms……42

Figure III.3. Daytime influence on average outlet temperature at different Re number……43

Figure III.4. Daytime influence on the PV cells' temperature at different Re number……..43

Figure III.5. Daytime influence on the panel's electrical efficiency at different Re number……44

Figure III.6. The influence of diurnal radiation on the panel's thermal efficiency at different Reynolds number……..45

Figure III.7 (a) velocity contours and (b) thermal fields as a function of solid layer height (h= 0 to 0.7) for Re = 1000 and solar radiation (ϕ = 1000W/m^2).

(a) velocity contours……46

(b) Isotherms……47

Figure III.8. Velocity profile for different values of h……..48

Figure III.9 (a) velocity contours (b) and thermal fields as a function of solid layer length (l = 0 to 0.75L) for Re = 1000 and solar radiation (ϕ = 1000W/m^2).

(a) Velocity contours……48

(b) Isotherms……48

Figure III.10. Velocity profile for different values of l……..50

Figure III.11. Graphical interpretation of the impact of the variation of h and l on the electrical efficiency……...51

Figure III.12. Graphical interpretation of the impact of the variation of h and l on the thermal efficiency……...51

List of Tables

Chapter I

Table I.1. Conversion efficiencies of various PV module technologies……12
Table I.2. Temperature coefficients of different PV technologies……13

Chapter II

Table II.1. Specifications of the studied PVT……...31
Table II.2. Thermal Properties of the studied PVT module…….31
Table II.3. Dimensional thermal and dynamic boundary conditions……32
Table II.4. Validation of the asymptotic values of the Nusselt number……37

Chapter III

Table III.1. Average solar radiation levels throughout daylight hours in summer……40

Nomenclature

Dimensional Quantities		
Symbol	Meaning	Unity
T	Temperature	K
T_0	Inlet temperature	K
T_{out}	Outlet temperature	K
T_{PV}	Average cell temperature	K
p	Pressure	Pa
H	Fluid canal height	m
L	Fluid canal length	m
h	Solid layer height	m
l	Solid layer length	m
u	Velocity x-component	m/s
v	Velocity y-component	m/s
u_0	Channel entry velocity	m/s
A_c	Solar panel surface	m^2
Q_u	Useful thermal energy	J
ϕ	Solar radiation intensity	W/m^2
Cp	Specific heat	J/kg.K
ρ	Density	kg/m^3
μ	Dynamic viscosity	Pa.s
k	Thermal conductivity	W/mK
$\dot{m}$	Mass flow rate	kg/s
η_{Th}	Thermal efficiency	%
η_{El}	Electrical efficiency	%
Dimensionless quantities		
Re	Reynolds number	-
Pr	Prandtl number	-
P	Dimensionless pressure	-
θ	Dimensionless temperature	-
U	Dimensionless x-component velocity	-

V	Dimensionless y-component velocity	-
Abbreviations		
PV	Photovoltaic	-
PVT	Photovoltaic thermal	-
AC	Alternating current	-
DC	Direct current	-
EVA	Ethylene vinyl acetate	-
CIGS	Copper Indium Gallium Selenide	-
CdTe	Cadmium Telluride	-
a-Si	Armophous silicon	-
TMS	Thin flat metallic sheet	-
PCMs	Phase change materials	-

General Introduction

General Introduction

Energy is vital for human life, powering everything from lighting to machinery. While crucial, many energy sources negatively impact the environment, thereby threatening human well-being. Balancing environmental protection with energy needs necessitates exploring both renewable and non-renewable options. Currently, non-renewable fossil fuels (coal, oil, gas) dominate global energy production (over 80%), but their greenhouse gas emissions, like carbon dioxide (CO_2), cause climate change and related disasters like droughts and cyclones. Conversely, renewable sources like solar, wind, and hydropower offer environmentally friendly alternatives. **[1]**

The global energy landscape is undergoing a profound transformation, driven by the urgent need to mitigate climate change and ensure sustainable energy security. Renewable energy sources, particularly solar energy, are playing an increasingly crucial role in this transition. Photovoltaic (PV) technology, which directly converts sunlight into electricity, has witnessed remarkable advancements in recent years, leading to a significant decrease in costs and a substantial increase in efficiency. On the other hand, solar thermal collectors harness the sun's energy for heating purposes. However, the inherent limitations of PV systems, such as their relatively low efficiency and the significant amount of heat generated, continue to present challenges in achieving optimal performance and widespread adoption.

Efforts by researchers to enhance the efficiency of PV collectors led to the development of photovoltaic thermal (PVT) solar panels. PVT panels combine the functions of traditional PV panels and solar thermal collectors, enabling the simultaneous generation of electricity and heat. This dual functionality significantly increases the overall energy efficiency of the system and opens up new possibilities for various applications, including domestic hot water heating, space heating, and industrial process heat. The efficiency of a PVT system is heavily influenced by several factors, including the design and configuration of the fluid flow passage within the panel. Effective heat transfer is paramount for maximizing both the electrical and thermal outputs of the system. **[2]**

This thesis investigates the optimization of an air-based PVT solar collector performance through a novel approach focusing on the strategic reduction of the flow passage section. Conventional PVT panel designs often feature relatively large flow channels, which, while facilitating ease of fluid flow, can compromise the efficiency of heat transfer from the PV cells to the coolant. A reduced flow passage, on the other hand, can lead to increased fluid velocity

and enhanced convective heat transfer, potentially resulting in improved electrical and thermal efficiencies.

This document is subdivided into three following chapters, followed by a general conclusion:

- **Chapter 1:** Provides a foundational overview of renewable energy, tracing the development of photovoltaic thermal (PVT) systems from photovoltaic (PV) and thermal collector technologies. The chapter concludes with a comprehensive review of advancements in PVT technology.

- **Chapter 2:** Focuses on the design and analysis of an air-based PVT solar collector. It details the geometric design, the physical model, and the specific boundary conditions used in this research. The chapter then presents the numerical analysis, including a discussion of mesh effects and the validation of our FORTRAN code.

- **Chapter 3:** Presents the results of the numerical simulations, along with observations and discussions for two distinct scenarios. The first scenario examines the impact of varying Reynolds numbers and time of day on the PVT system's performance. The second one investigates the effect of a solid layer of variable dimensions inserted at the channel exit, while maintaining constant Reynolds number and radiation levels.

Finally, a general conclusion summarizes the key findings presented throughout the document.

Chapter I

Introduction to Renewable Energies and the Photovoltaic Thermal Technology

Chapter I

I.1 Introduction

This chapter lays the groundwork for this research on “Optimization of the performance of a thermal photovoltaic solar panel by reducing the flow passage section.” We'll start by taking a look at the world of renewable energy, understanding its importance and how it impacts our daily lives.

Renewable energy stands in contrast to fossil fuels, which are non-renewable within our generation time. Often called "green energy", renewable sources like solar and geothermal energy are environmentally friendly because they produce energy without releasing harmful greenhouse gases that contribute to climate change.

These renewable energy sources ultimately trace back to two primary sources: the sun and the earth. Natural processes like evaporation, condensation, and the decomposition of organic matter lead to various forms of renewable energy, such as wind, geothermal, and biogas.

Before delving into the thermal photovoltaic systems, we'll first explore the two foundational technologies that paved the way: photovoltaic panels and thermal panels. By understanding these individual technologies, we'll gain a solid foundation for appreciating the unique capabilities of thermal photovoltaic panels.

Lastly, we'll examine the driving forces behind their development, highlighting their advantages over the traditional PV systems. Finally, we'll provide a comprehensive list of bibliographical references for further exploration.

I.2 Renewable Energies

Unlike fossil fuels, which take millions of years to form, renewable energy sources replenish themselves within our lifetime. Renewable energy sources and fossil fuels are both crucial for our daily energy needs such as powering our homes with electricity and heat and propel our vehicles. The key difference lies in their formation time. Fossil fuels like oil, coal, and natural gas were slowly formed from the decomposition of organic matter, making them non-renewable. In contrast, renewable energies like solar and wind energy are rapidly replenishable.

Climate change has been a major catalyst for the widespread adoption of renewable energies. The goal of achieving net-zero CO_2 emissions has become a global priority, driven by the urgent need to address climate change. This pressing environmental issue, caused by a combination of natural and human activities, is characterized by a gradual increase in atmospheric temperatures. To quantify the impact of climate change, scientists measure pollution levels and express all climate-altering gases in terms of CO_2 equivalents. Many renewable energy sources, such as solar, wind, and wave energy, are completely CO_2-neutral when their production processes are not considered.

The rapid development of renewable energy technologies is a testament to their growing importance. It's safe to assume that these technologies will continue to evolve and improve in the years to come, playing a crucial role in shaping a sustainable future. **[3]**

I.2.1 Forms of renewable energies

It's important to remember that the world of renewable energy is diverse, with many different options like solar, biomass, wind, hydroelectricity, tidal, and geothermal power. Each of these technologies has its own strengths and weaknesses, making it crucial to consider the specific needs and conditions of each location when choosing the best renewable energy solution.

Solar power is a leading force in the global transition to clean energy, offering a powerful and sustainable source of green energy. Solar energy is captured through photovoltaic panels, which convert sunlight into electricity, and thermal solar collectors, which harness the sun's heat. This versatile energy source can be used both for heating and electricity generation.

Biomass is a renewable energy source derived from organic matter like plants and animals especially those which are no longer used for food or feed. Examples of biomass include wood and wood waste, agricultural crops and waste, food and yard waste, animal manure and also human sewage.

Today, wind turbines capture the power of the wind to generate electricity. Their working principle is quite simple. The wind spins the blades of the turbine, which are connected to a gearbox and then a generator. This rotation creates electricity.

Hydropower harnesses the power of flowing or falling water to spin turbines, like the watermills of the past or the modern dams we see today. The water’s kinetic energy strikes the

blades of a turbine causing them to spin. The spinning turbine, connected to a generator, drives it converting the mechanical energy into electrical energy.

Geothermal energy, on the other hand, is a sustainable source of heat that originates from the incredibly hot Earth's core. This heat can travel through channels of water or steam, making its way to the surface. It can be used for heating purposes without the need for specialized equipment. Apart from heating, it can also be harnessed to generate electricity using the turbine generator circuit.

Each of these renewable energy technologies has its own strengths and weaknesses, making it essential to carefully consider the specific needs and conditions of each location when choosing the best solution. **[4]**

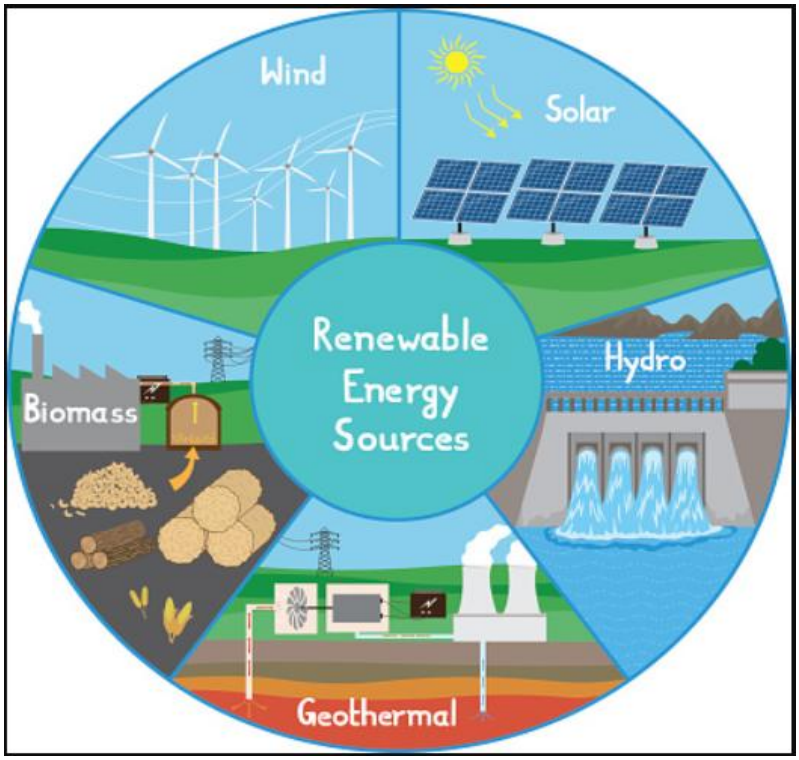


Figure I.1. *Different sources of renewable energies.**[5]***

I.3 Solar Collectors

This part of this chapter delves into two types of solar collectors: photovoltaic and thermal. It will provide an overview of key concepts related to these systems, including their individual components, materials used to make them and operating principles.

I.3.1. Photovoltaic Solar Collectors

I.3.1.1 *The photovoltaic effect*

The photovoltaic effect was discovered by the French physicist Becquerel in 1839. The word "photovoltaic" comes from the word "photo" (from the Greek "phos" which means "light") and the word "Volt" (the surname of the physicist Alessandro Volta who made a very important contribution to research in electricity). The photovoltaic effect is the direct conversion of energy from solar radiation into electrical energy by means of cells, usually silicon-based. To obtain sufficient power, the cells are connected to each other and form solar modules.

I.3.1.2 *An off grid Photovoltaic solar system*

In remote locations without access to the traditional power grid, photovoltaic solar modules can be a primary source of electricity. These modules can directly power essential equipment like lights and appliances.

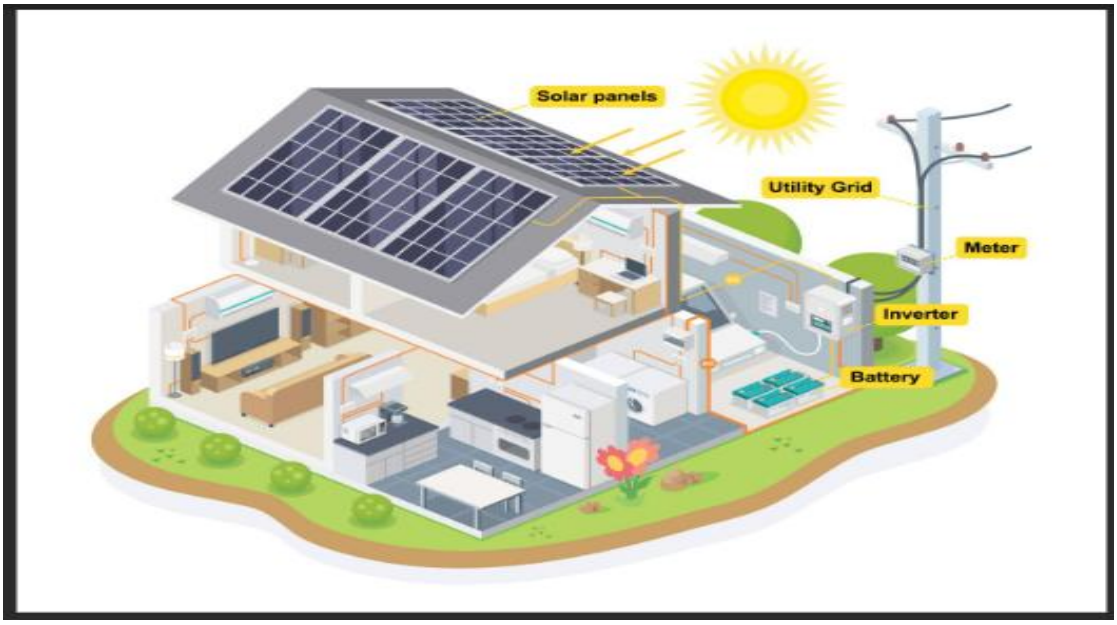


Figure I.2. *An off grid photovoltaic solar system* ***[7]***

To ensure continuous operation even when the sun isn't shining, batteries store the energy generated during daylight hours. This stored energy is stored in a chemical form, ready to be released when needed. For optimal battery performance and longevity, a charge controller is

crucial. It prevents overcharging, which can damage the batteries, and deep discharging, which can shorten their lifespan. In some isolated sites, appliances that require alternating current (AC) can be used. This necessitates the inclusion of an inverter, which converts the direct current (DC) generated by the solar panels into AC. If the solar system produces more electricity than needed, the excess energy can be fed back into the utility grid. This "excess" energy can be sold, and a meter is installed on the grid to accurately track the amount of energy supplied. **[6]**

I.3.1.3 *Principal components of solar PV modules*

While solar panels may appear as single units, they are actually intricate systems made up of several essential components working together harmoniously. A typical solar PV module, often referred to as a solar panel, is comprised of eight primary components, as illustrated in the diagram.

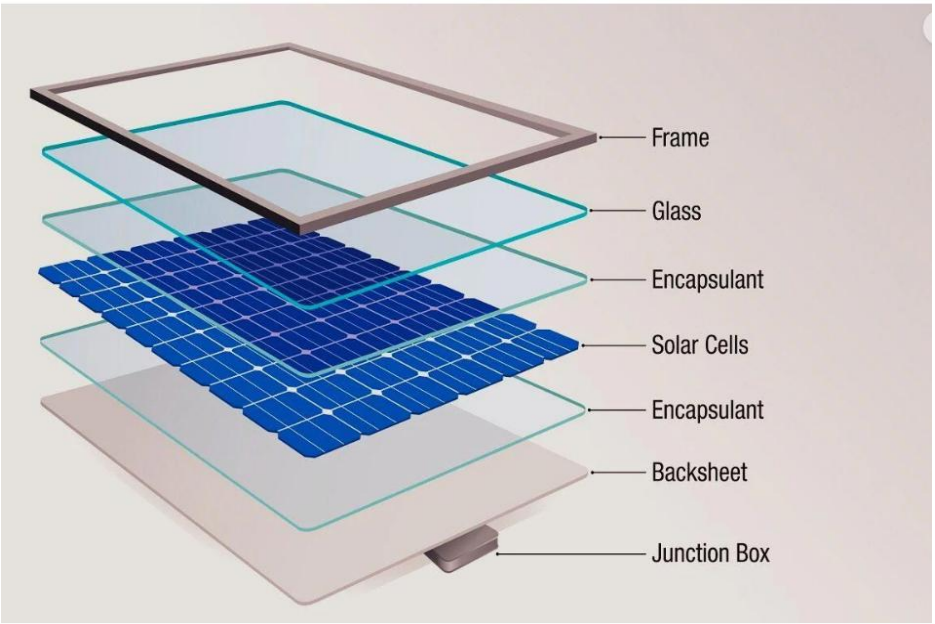


Figure I.3. *The main components of a PV module* ***[8]***

- ***Solar cells***

Solar cells are the fundamental building blocks of solar panels. They are responsible for the conversion of solar energy into electrical energy. Since a single solar cell produces very little amount of energy, numerous solar cells are combined together to create a single solar module.

- ***Solar glass***

Solar panels are vulnerable to harsh weather conditions like wind and dust. To protect them, solar glass acts as a shield, enhancing their performance. For optimal protection, solar glass should be durable and have reflective surfaces. Tempered glass, with a thickness between 3mm and 4mm, is a recommended choice.

- ***Back sheet***

It is used essentially as the panel back side protective layer. It protects the panel mechanically and electrically i.e. insulation.

- ***EVA (Ethylene Vinyl Acetate)***

The EVA, or ethylene vinyl acetate, is like a clear, protective shield for the solar cells. It's a highly transparent plastic layer that wraps around the cells, holding them together like a strong, laminated cover. This EVA is a tough cookie, able to withstand extreme temperatures and humidity without cracking or breaking.

- ***Aluminium Frame***

The aluminium frame is the secret weapon for these solar panels. It is robust, rigid, and lightweight, which means it is incredibly strong and can withstand a lot of pressure. This makes the panels able to handle harsh conditions like high winds and other external forces without a problem.

- ***Junction Box***

It sits on the backside of the panel and acts as the central hub for all the cables connecting to the solar panels. It's like the control centre for the electrical system, ensuring all the connections are secure and preventing any electrical hazards. **[8]**

I.3.1.4 *Interconnection between PV Modules*

PV modules can be combined in series, parallel or mixed configuration, depending on the desired outcome. In series connection, the resulting voltage is the sum of each cell added together leaving the current unchanged. In parallel connection it is the opposite. This connection makes it possible to add the currents while maintaining the voltage constant.

However, these two configurations can be mixed. This configuration is useful when a certain power is needed at a desired voltage. These three possible configurations are also applicable for the interconnection between cells to make up a module.

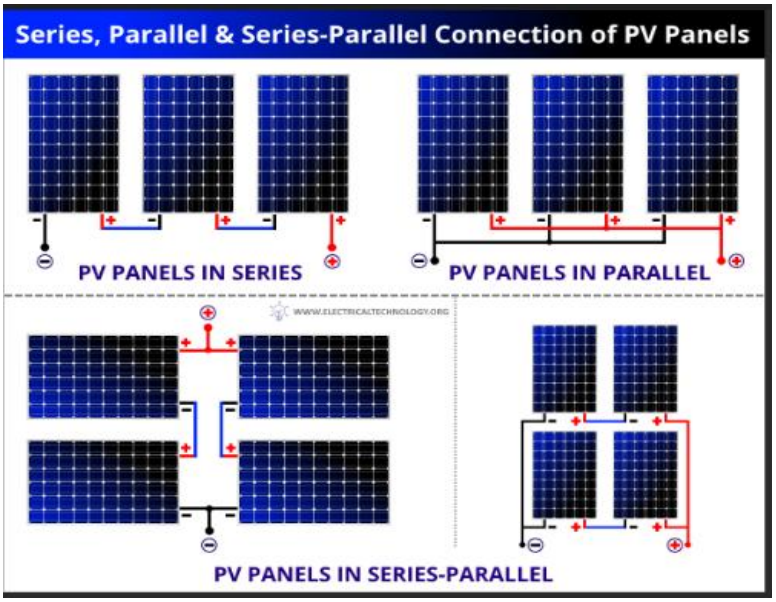


Figure I.4. *Series, parallel and mixed configuration of solar PV modules* ***[9]***

I.3.1.5 *Working Principle of a PV Cell*

A photovoltaic cell, or solar cell, transforms the power of the sun to electricity. This process relies on the photovoltaic effect, where light striking the cell's surface creates an electrical current. The voltage produced by a single cell typically ranges from 0.3 to 0.7 volts. This depends on factors like the materials used to make the cell, the arrangement of the cells, as well as the cells' operating temperatures and age.

A photovoltaic cell is based on the following three mechanisms: Absorption of photons (whose energy is greater than the gap) by the material constituting the device; Conversion of photon energy into electrical energy, which corresponds to the creation of electron/hole pairs in the semiconductor material; collection of particles generated in the device. The material making up the photovoltaic cell must therefore have two energy levels and be conductive enough to allow the flow of current: hence the interest of semiconductors for the photovoltaic industry. In order to collect the generated particles, an electric field is required to dissociate the electron/hole pairs created. **[6]**

I.3.1.6 *Types of PV cells*

Crystalline silicon, which accounts for the majority of PV cell production; and thin film, which is newer and growing in popularity, are the two main technologies which are dominating the Photovoltaic industry. Crystalline cells are made from ultra-pure silicon raw material such as those used in semiconductor chips. In this case, silicon wafers are sliced into thin sheets that are typically in the range of one fifth of a millimetre thick. Thin film is made by depositing layers of semiconductor material barely 0.3 to 2 micrometres thick onto glass or stainless-steel. The costs of raw materials are much lower than the capital equipment and processing costs due to the fact that solar cells are made from thin silicon semi-conductors.

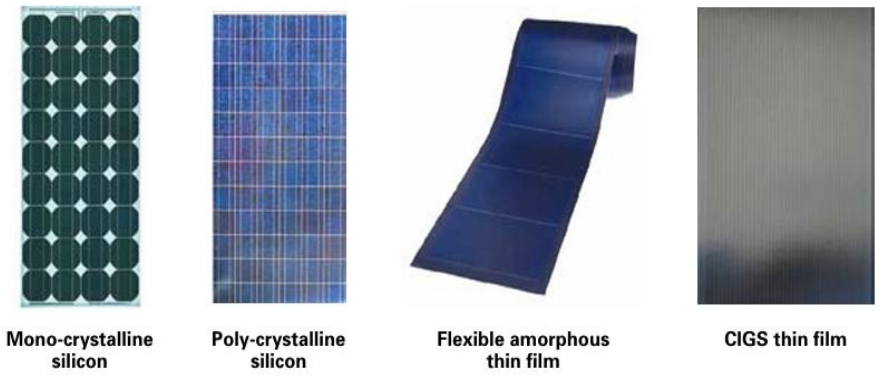


Figure I.5. *Common PV module technologies* ***[10]***

The benefits of each technology compared to the others stem from various factors: some technologies are more cost-effective, others boast longer lifespans, and some offer superior efficiencies. Below is a table that illustrates the efficiencies of different technologies, summarizing the conversion efficiencies of the aforementioned technologies.

Table I.1. *Conversion efficiencies of various PV module technologies* ***[10]***

Technology	Module Efficiency (%)
Mono-crystalline	12.5 – 15
Poly-crystalline	11 – 14
Copper Indium Gallium Selenide (CIGS)	10 – 13
Cadmium Telluride (CdTe)	9 – 12
Amorphous Silicon (a-Si)	5 - 7

I.3.1.7 *Effect of Temperature on PV Solar cells*

While it's tempting to think that hotter temperatures mean more energy from PV solar panels, that's only true for thermal solar panels. With photovoltaic (PV) solar panels, the relationship is more complex. As the temperature increases, the energy output initially rises, but only up to a certain point. After that, the energy output starts to decline as the temperature continues to rise.

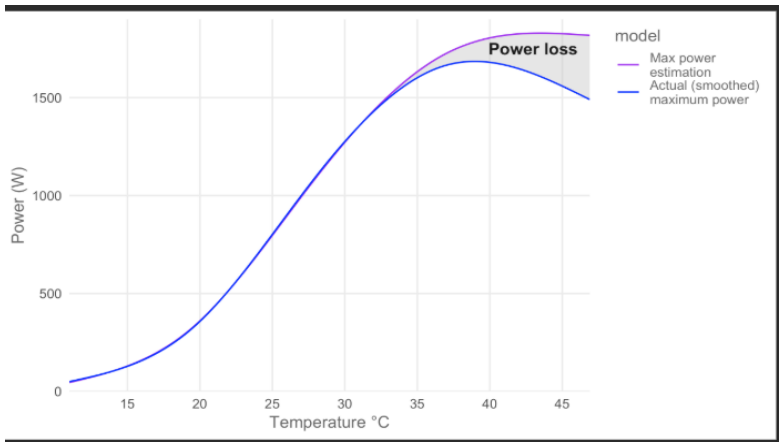


Figure I.6. *Effect of temperature on the Power output of PV cell* ***[10]***

An experiment was carried out in Singapore under the blazing sun. The temperature of the cells can soar to over 70°C, while most PV modules are designed to perform best at 25°C. This difference in temperature can significantly impact the energy output. The power loss at 70°C is calculated by multiplying the temperature difference (70°C - 25°C = 45°C) by the temperature coefficient of the panel. This coefficient tells us how much the panel's output changes for every degree Celsius increase in temperature. Interestingly, thin film technologies generally have a lower negative temperature coefficient compared to crystalline technologies. This means they lose less of their rated power output as the temperature rises. In simpler terms, they are more resilient to the negative effects of high temperatures. **[10].**

Table I.2. *Temperature coefficients of different PV technologies* ***[10]***

Technology	Temperature coefficient (%/°C)
Crystalline Silicon	-0.4 to -0.5
CIGS	-0.32 to -0.36
CdTe	-0.25
a-Si	-0.21

I.3.2. Thermal solar collectors

I.3.2.1 *Commercial thermal solar collectors*

Thermal solar systems are designed to harness the sun's energy by concentrating its radiation to generate high temperatures. This heat is then used to power thermal machines. The two main types of generators providing high power are based on direct (or indirect) radiation from the sun. Direct radiation systems capture sunlight directly then convert it into heat while indirect radiation systems utilize mirrors or lenses to focus sunlight onto a central point, creating concentrated heat. The accumulated heat can be used for two main purposes: heating domestic water and buildings, or generating electricity. The electricity generation is achieved by using the heat to vaporise water forming steam, which then drives turbines connected to a generator, ultimately producing electricity.

This technology has several remarkable advantages. The first is the storage of Energy in the form of heat that can be used during the night. Secondly, is the possibility of growing below the panels since they are installed 3 to 5 meters above the ground. However, these systems are best suited for regions with abundant sunshine. Cloudy skies significantly reduce their effectiveness, limiting their applicability in certain climates. These technologies stand out for their high efficiency compared to other renewable sources. Their thermal efficiency ranges from **20% to 40%**, while their electrical efficiency sits between **13% and 25%**. Furthermore, they are capable of producing significant amounts of energy, reaching hundreds of Megawatts. **[6,11]**



Figure I.7. *Parabolic solar collectors* ***[12,13]***

I.3.2.2 *Domestic thermal solar collectors*

Thermal solar heating, while often used for large-scale electricity generation, can also be effectively implemented for smaller, domestic applications like heating domestic water and buildings. This direct use of absorbed heat for warmth eliminates the need for electricity conversion. These applications utilize flat-plate collectors, which are made of glass with a translucent coating that allows sunlight to pass through. The backside absorber sheet absorbs the heat and transfers it to a circulating fluid via copper tubes. This fluid then carries the heat for use. These collectors typically reach temperatures up to 75 degrees Celsius, though higher temperatures can be achieved with high-efficiency models.

There are two main types of flat-plate collectors based on the heat transfer fluid: liquid and air. These collectors are mostly mounted on rooftops of buildings. They are simple to maintain and don't require tracking of the sun's movement. **[14,15]**



Figure I.8. *Domestic thermal solar collectors* ***[16]***

I.3.3. Photovoltaic Thermal Solar Collectors

I.3.3.1 *Description*

This chapter has earlier addressed the effect of temperature on the overall power output of PV solar panels. While energy output initially increases with temperature, it eventually starts to decline as illustrated by **Figure 1.6**. In areas like deserts, where solar radiation is intense during summer, higher operating temperatures of PV cells can reduce their lifespan.

To address the challenges of temperature-related efficiency and lifespan issues in solar panels, researchers have developed Photovoltaic Thermal (PVT) systems. These hybrid systems combine photovoltaic (PV) cells with thermal technologies. In PVT systems, the PV cells are integrated directly into the thermal absorber plate. This plate is attached to a heat exchanger where a circulating heat transfer fluid absorbs and carries the thermal energy. This innovative design allows sunlight to be converted into both electrical and thermal energy within a single module. PVT systems offer significant advantages over using PV or thermal technologies individually. Their dual functionality leads to greater overall solar energy conversion, improving resource utilization. Additionally, the cooler heat transfer fluid helps to reduce cell temperature, thereby boosting electrical efficiency and extending the lifespan of the solar cells **[17,18]**.

System calculations to compare the efficiencies of the hybrid solar collector to the individual technologies were carried out and the results were as follows: A combined PVT collector, with a 2m² area, generated 720 kWh of thermal and 132 kWh of electrical energy. This hybrid collector outperformed two separate 1m² collectors (one for domestic hot water, one photovoltaic), which yielded only 520 kWh thermal and 72 kWh electrical energy respectively. The PVT system produced approximately 44% more energy overall. While beneficial in most areas, this increased energy yield per square meter is especially advantageous in densely populated regions. **[19]**

I.3.3.2 *Different Types of PVT modules*

PVT modules can be categorized in various ways. Common classifications include the type of heat transfer fluid used, the type of photovoltaic cells employed, and how they are integrated onto rooftops. This section will focus on classifying PVT modules based on the heat transfer fluid: air-based and water-based systems.

- ***Air-based***

As the name suggests, air-based PVT modules are solar heating systems that incorporates an additional layer of photovoltaic material laminated either above or below mechanically or naturally ventilated air ducts. The air flow in this configuration cools the PV cells by absorbing the waste heat energy from the cells thereby enhancing the overall functionality of the modules. This design can involve air flowing above, below, or both above and below the

PV modules. These modules may or may not have a glass cover, with options for single or double glazing. The module's backside insulator acts as a barrier to prevent heat dissipation from the PVT system. The primary function of air-based PVT modules is to provide multiple benefits simultaneously: generating electricity, supplying heated air for space heating or other applications such as agricultural drying, and improving ventilation. The versatility of this technology makes it suitable for a wide range of users and applications. The figure below illustrates the possible types of air PVT modules.

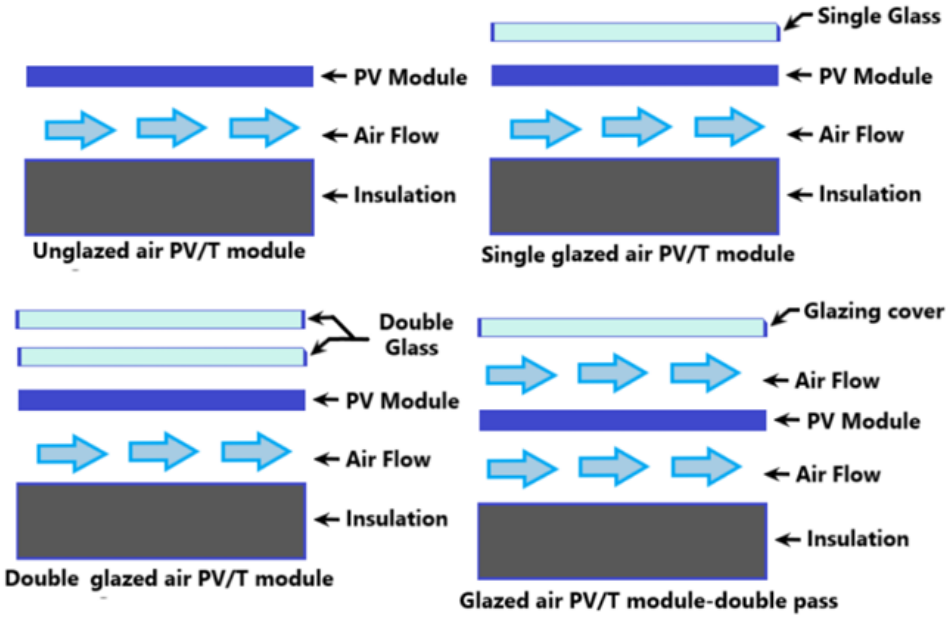


Figure I.9. *Possible configurations in air-based PVT modules.**[17]***

- ***Water-based***

Water-based PV/T modules, similar in design to traditional flat-plate solar collectors, use PV cells integrated into a water-carrying system. Water flows through pipes or coils positioned beneath the PV cells. This flowing water acts as a coolant, particularly effective when water temperatures are low. This cooling effect helps improving the PV cells' electrical efficiency. The water absorbs heat from the PV cells, becoming heated and usable for other purposes. Multiple layers of water flow are possible, and some designs incorporate both water and air for enhanced cooling. Excess heated water can be used directly or cooled before recirculation to recover additional heat. Compared to air-based systems, water-based PVT systems offer superior cooling due to water's higher thermal mass, resulting in significantly improved thermal and electrical efficiency. **[17]**

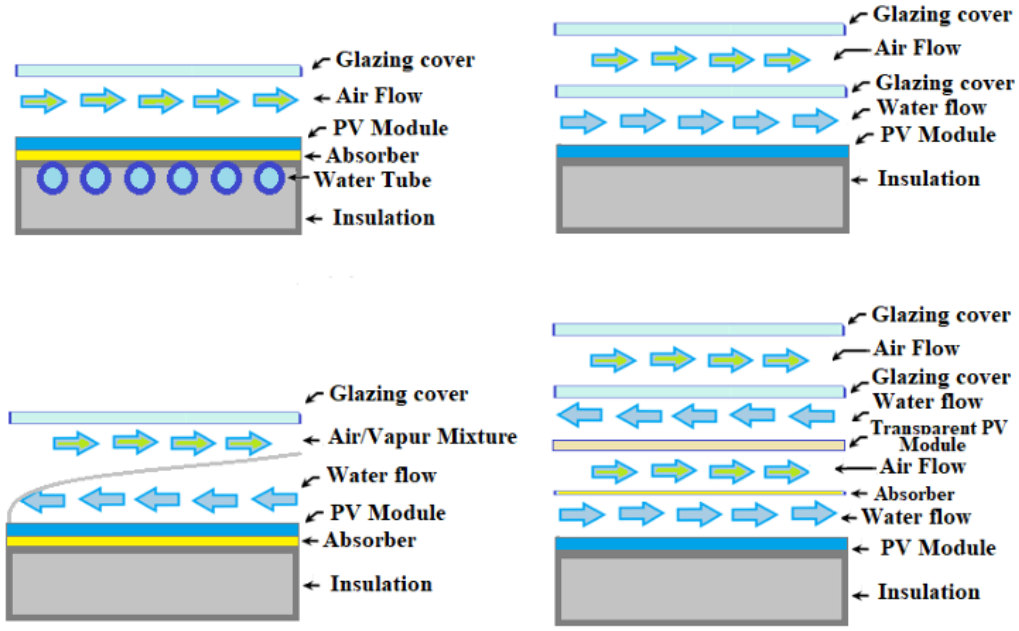


Figure I.10. *Possible configurations in water-based PV/T modules.**[17]***

I.3.4. Bibliographic Research on PVT Systems

I.3.4.1 *History of PVT systems*

The PVT concept has been in existence for close to five decades now and has been discussed by numerous publications. The first works on the PVT systems were conducted by **Wolf [20]**. An analysis of the performance of these combined systems on a single-family residence for the whole year was carried out. The results showed that the combination of these two systems, PV and thermal was technically feasible and cost effective. **Florschuetz, 1979 [21]** conducted a theoretical study of PVT systems through Hottel Whillier–Bliss equation to model PVT systems, where a linear decreasing relationship between the cell efficiency and its operating temperature was proposed. Later in **1985, Cox and Raghurman [22]** developed simulation software to allow the study of hybrid PVT performances and emphasized the influence of optical properties of glazing on the thermal and electric efficiencies. In order to eliminate the need for an external electrical power source to drive the circulation pump in conventional solar thermal systems, **Bhargava et al. [23]** proposed a hybrid system in **1991**. This innovative design, combining thermal and photovoltaic technologies, aimed to generate sufficient electricity to power the pump. However, results indicated that self-sufficiency depended upon specific design parameters and flow rates.

In **1994, Jai Prakash [24]** conducted a theoretical study to compare the performance of a conventional PV panel with that of a hybrid photovoltaic-thermal (PVT) solar system. In order to extract heat from the system there by cooling the PVT solar cells, air/water is made to flow in a duct placed below the surface on which the solar cells are mounted. The (PVT) system consisted of a single glazing of 3 mm thick glass sheet. When water is used as the heat recovery fluid, the duct inlet was connected directly to a tap, but when air was used, a pump was employed for the air to flow through the duct. Results of this study showed that, as the flow rate increases for both configurations, with air and water, the thermal efficiencies also increase. For water heating the thermal efficiency varies between 50 and 67%, while for air heating, it varies between 17 and 51%. The lower thermal efficiencies in the case of air heating were due to poor heat transfer between the absorber plate and the flowing air.

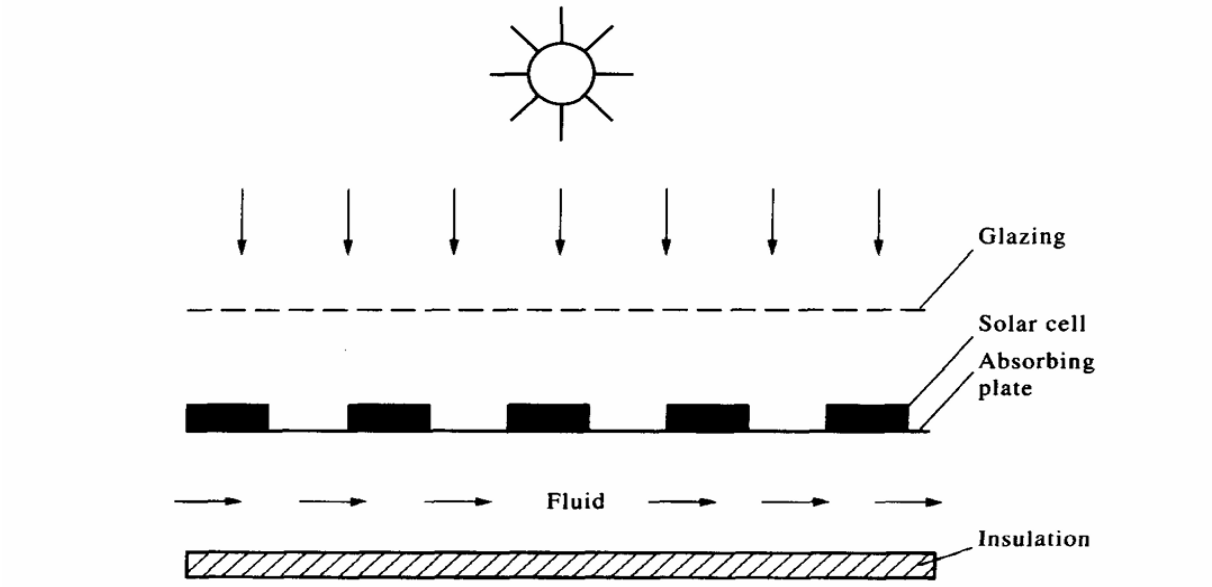


Figure I.11. *Design of the solar photovoltaic/thermal (PVT) air/water heating system* ***[24]***

A comparison between a PVT collector and a pure thermal absorber was carried out by **Sandnes and Rekstad [25]** in **2002.** The water-based PVT system used in the experiment was made by combining a polymer solar heat collector, made of a black plastic solar heat absorber, with single-crystal silicon PV cells. Thermal efficiency measurements for these different configurations showed reduced thermal efficiency for the PVT system. This conclusion was attributed to:

- Available solar energy for the thermal system reduced by the fraction of the incident energy converted to electricity by the PV cells.

- A lower optical absorption in the PV cells compared to the black absorber plate
- Increased heat transfer resistance introduced in the cell/absorber interface.

On the other hand, cooling of the PV cells was achieved which increased the cells' efficiency due to the use of the heat transfer fluid, water.

In **1996**, **Sopian et al. [26]** conducted a comparison of the performances of two air-based PVT systems: a single-pass and a double-pass, using steady-state models. The performance analysis indicated that the double-pass photovoltaic thermal solar collector outperformed the single-pass model within the typical operating mass flow rate range. This double-pass configuration led to reduced cell temperatures and lower glass cover temperatures, which in turn enhanced both the electrical and thermal efficiencies.

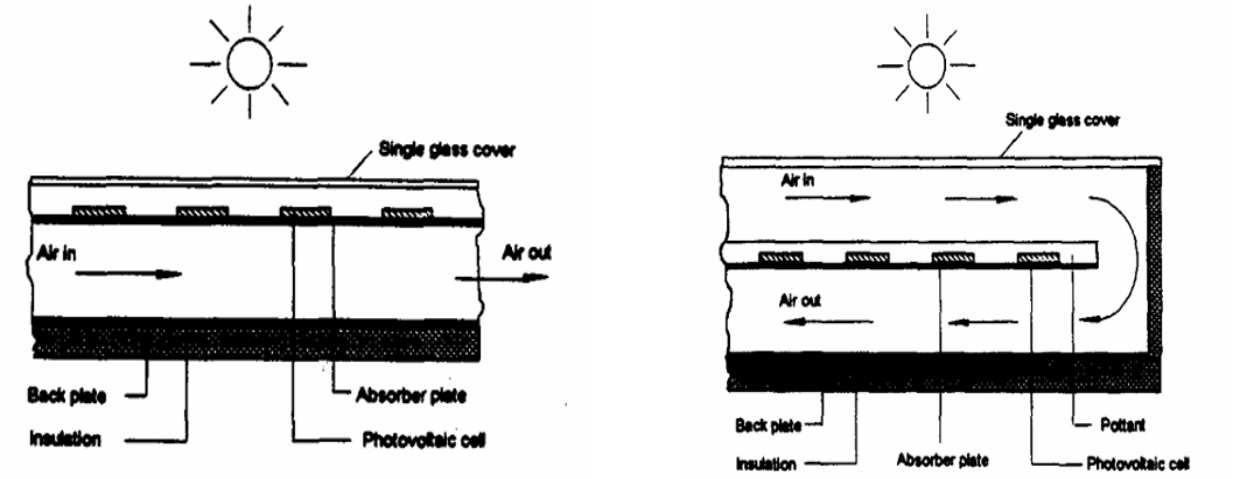


Figure I.12 *Configurations of the single-pass and the double pass PVT collectors* ***[26]***

In 2003, **Nagano et al**. **[27]** conducted an experimental analysis in order to evaluate the electrical power generation and solar heat collection capabilities of six different types of experimental thermal-PV hybrid wallboards. They developed hybrid PVT exterior wallboards incorporating PV cells inclined at an angle of 80 degrees and an air gap for heat evacuation as shown in figure 1.10. Different cell technologies, amorphous and polycrystalline silicon, protected by either glass cover or Teflon film were used in this study. The results showed higher conversion efficiency for polycrystalline cells relative to amorphous silicon cells, 11% and 3% respectively. The average thermal collector efficiency ranged from 20.2% to 22.3% for wallboards without glass covers and from 29.2% to 36.9% for those with glass covers for the outside air temperature of 0C.

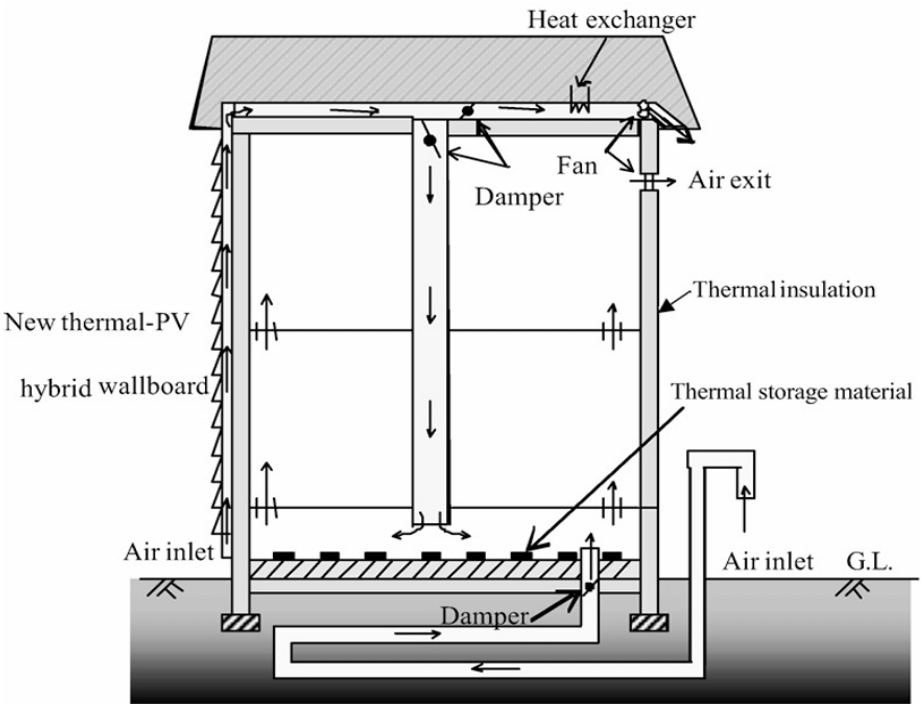


Figure I.13. *The structure of the building incorporated with hybrid wallboard.**[27]***

For the past few years, an increasing number of theoretical, experimental and numerical studies have been conducted to analyse and improve the performance of the PVT systems using different structural designs and cooling techniques. In this context, structural designs play a crucial role in improving the performance of PVT collectors. Many structural designs aim to maximize contact between the PV absorber and the heat transfer fluid thereby increasing the heat evacuation rate. **Tonui and Tripanagnostopoulos [28],** used a suspended thin flat metallic sheet, TMS, at the middle of an air flow canal and fins at the back wall of an air duct as heat transfer augmentations in an air-cooled solar collector. The steady-state thermal efficiencies of the modified systems were compared with those of typical PVT air system. The experimental analysis on the three different models is shown in figure 1.11. The results obtained showed that, with a forced convection flow rate of 60m3/h and a 15cm channel depth, the configuration with fins resulted in the highest thermal efficiency at 30%, followed by the TMS at 28%, and lastly the typical system at 25%. This suggests that the modifications made improved thermal efficiency compared to the standard system. Additionally, the PV cooling achieved with these modifications led to better electrical performance. Both modified systems exhibited lower back wall temperatures than the reference system, with the TMS system showing the lowest temperature due to the added shading effect of the suspended metallic sheet.

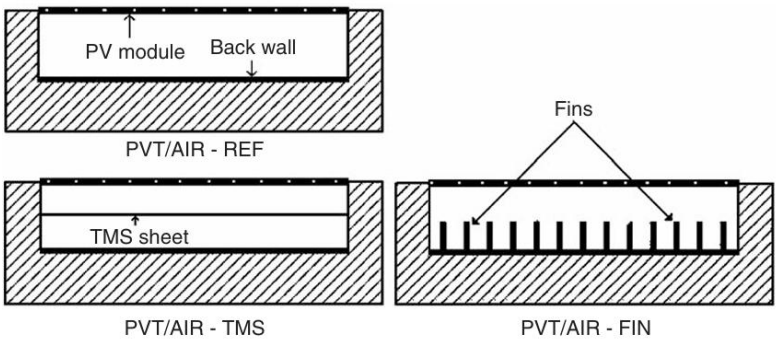


Figure I.14. *Cross-sectional view of PVT/AIR collector models. Fluid flow is perpendicular to the page* ***[28]***

In **2010, Jin et al. [29]** studied a modified air hybrid PVT system where the absorber had been changed to a rectangular tunnel and compared it with a system without a tunnel. The final results showed that the electrical, thermal, and overall efficiency of this modified system were 10.02%, 54.70%, and 64.72% respectively, which proves that the modified system had better electrical efficiency than the system without a tunnel. On the other hand, they observed that the surface temperature of the PV module decreases with the increase in the air flow rate passing through the rectangular tunnel.

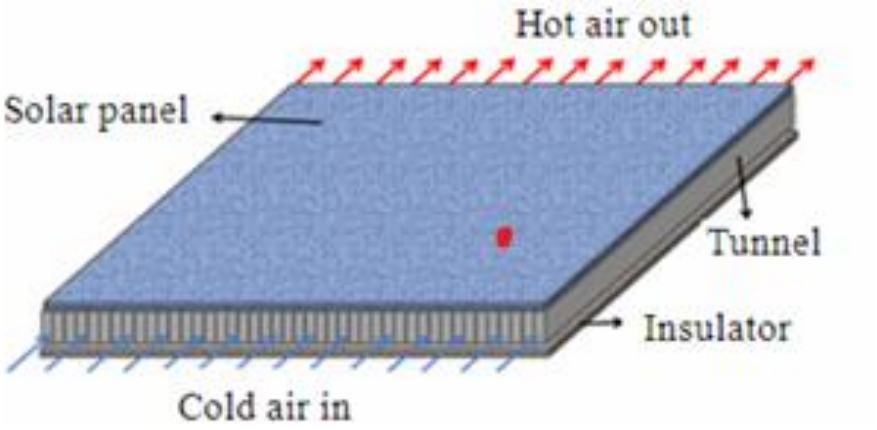


Figure I.15. *Solar Photovoltaic thermal air collector equipped with tunnels* ***[29]***

The study of **Othman et al. [30]** in **2013,** using stainless-steel wool, a honeycomb and a V-groove heat exchanger showed the convenience of a larger heat exchange surface. The thermal efficiencies were 71%, 86% and 87% while the electrical efficiencies were 7.04%, 6.88% and 7.13%, for the system with V-groove, stainless steel wool and with honeycomb respectively. The highest efficiency of the model with a honeycomb heat exchanger can be

attributed to its large surface area touching the back of the PV module and its ability to make air flow uniform thereby enhancing the heat transfer from the back of the PV module to the flowing air.

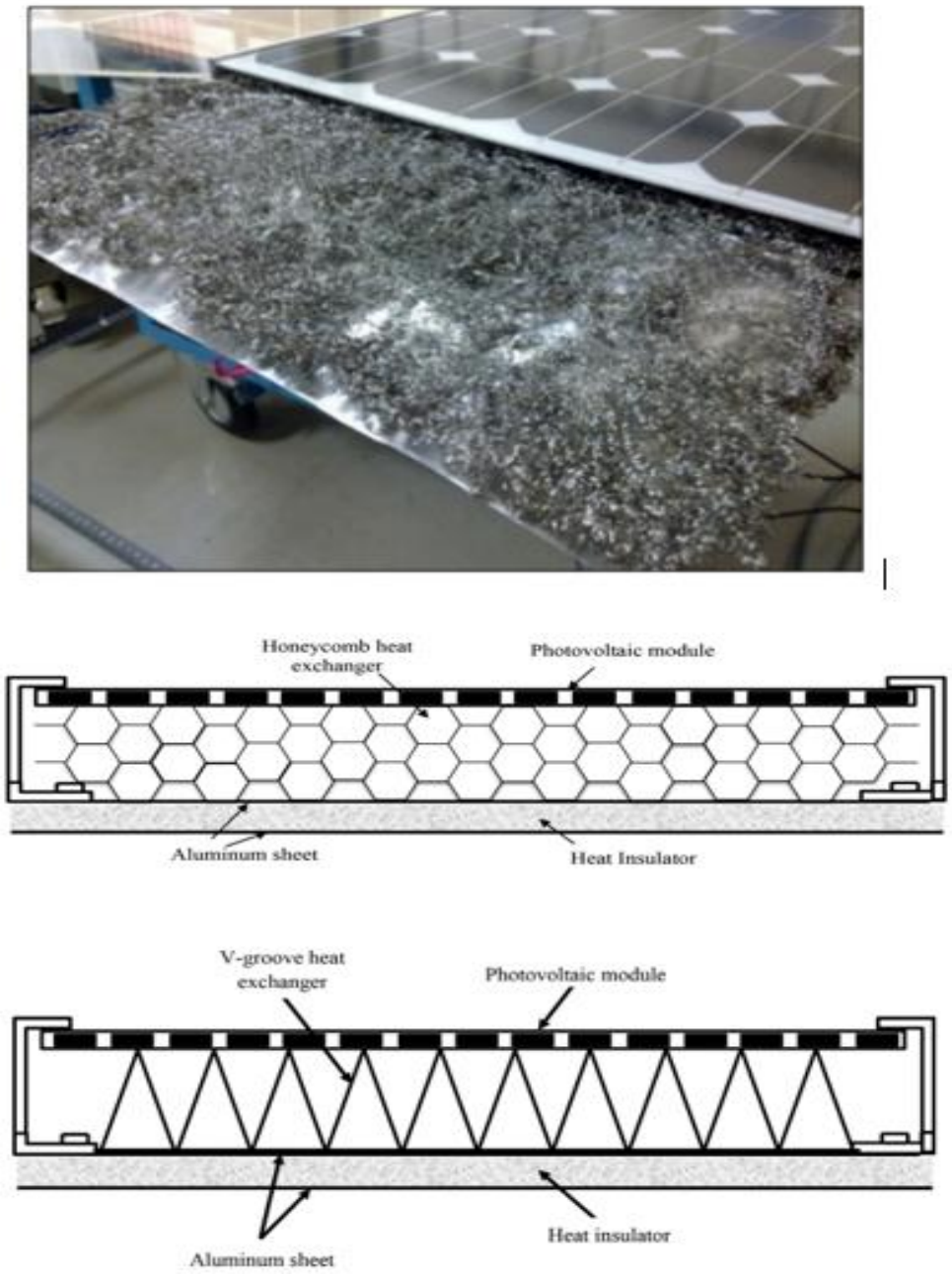


Figure I.16. *PVT collector with stainless-steel wool, honeycomb and V-groove heat exchangers* ***[30]***

Other structural designs focus on enhancing cooling both above and below the PV cells. Some designs also incorporate glass covers to protect against adverse weather and minimize

heat loss to the ambient environment. In this context, **Slimani et al. [31]** in **2019,** conducted a comparative study in Algiers Algeria using four monocrystalline solar device configurations: photovoltaic module (PV-I), conventional hybrid solar air collector (PVT-II), glazed hybrid solar air collector (PVT-III) and glazed double-pass hybrid solar air collector (PVT-IV). With an air flow rate of 0.023 kg/s the numerical results showed that the daily average overall energy efficiencies reached 29.63%, 51.02%, 69.47% and 74% for the first (PV-I), the second (PVT-II), the third (PVT-III) and the fourth (PVT-IV) configurations respectively during a sunny day in summer. It was also found that glazed hybrid collectors (PVTIII) and (PVT-IV) yielded relatively less electrical power compared to unglazed collectors (PV-I) and (PVT-II) while the double pass collector had better electrical efficiency than a single pass for the glazed configurations.

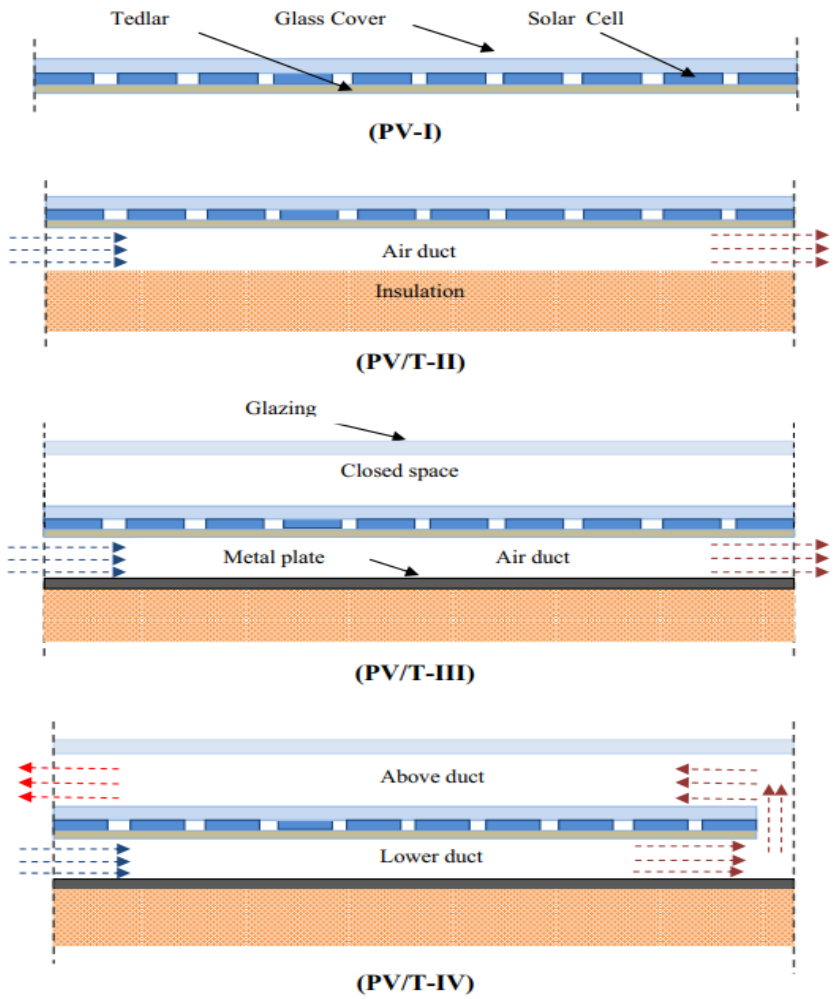


Figure I.17. *Schematic cross-sectional view of: photovoltaic module (PV-I), basic solar PVT air collector (PVT-II), glazed solar PVT air collector (PVT-III) and glazed double-pass solar PVT air collector (PVT-IV)* ***[31]***

Cooling techniques also play a significant role in increasing the energy efficiency of PVT panels. Reducing the temperature of the collectors improves the energy conversion efficiency of photovoltaic cells and enhances the performance of thermal energy collection. The use of nanofluids presents one of the advanced cooling techniques. Nanofluids are formed by the dispersion of nanoparticles, usually metal oxides to the base fluid. The nanoparticles help to boost the thermal conductivity of the base fluid thereby improving the heat transfer.

In **2018, Hosseinzadeh et al. [32]** conducted a study to assess the electrical and thermal energy efficiencies of a nanofluid-based photovoltaic thermal (PVT) system using, ZnO/water as the nanofluid. They employed ANSYS Fluent software, validating their results by comparing the simulation data with experimental measurements. The experiments took place on selected days in August and September at Ferdowsi University of Mashhad, Iran. The results of this study showed that the PVT with a nanofluid outperformed the water-based one. Notably, lowering the coolant inlet temperature from 40 °C to 20 °C improved the thermal energy efficiency of the nanofluid-based PVT system by 16.21%, while the electrical energy efficiency exhibited only slight variations.

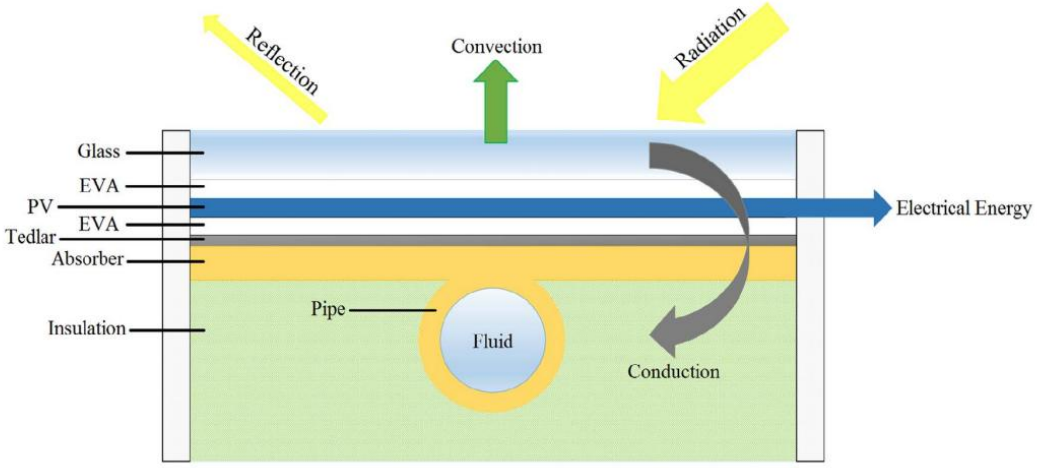


Figure I.18 *Schematic diagram of the nanofluid PVT system* ***[32]***

In the following year, **Joo et al. [33]** compared a standard water-based PVT system to two nanofluid PVT systems using CuO/water and Al2O3/water. With an optimal flow rate of 3 L/min (determined for the water-based system), the findings of this study showed significant thermal efficiency improvements over the standard system. It showed 21.30% for CuO/water and 15.14% for Al2O3/water. However, electrical efficiency gains were negligible, possibly

due to the small PV sample size or measurement errors. CuO/water showed a minor 0.07% increase, while Al2O3/water showed no change.

Phase change materials (PCMs) are also used in modern PVT technology to cool PVT systems and manage cell temperatures. As their name suggests, PCMs are substances that undergo phase change while they are in use. They can absorb, store and release large amounts of thermal energy during their melting and solidification. Where thermal stability is needed, PCMs plays a crucial role in stabilizing the temperatures since the phase change takes place at constant temperature. In order to allow efficient heat evacuation, PCMs are incorporated into a PV cooling system as either encapsulated or embedded in modules or heat sinks that are in direct contact with the PV cell.

Alsaqoor et al. [34] in **2023** examined the impact of incorporating PCMs in PVT systems and their electrical and thermal performance. A MATLAB Simulink code was developed, aimed at exploring the effect of solar irradiation and coolant mass flow rate on the electrical and thermal efficiencies of a standard PVT and a PVT with PCMs, PVT-PCM. Although the electrical efficiency of both configurations could be enhanced by increasing the mass flow rate, which improves the cooling of the photovoltaic cells, the PVT system with PCM was capable of lowering cell temperatures by 24% and enhancing electrical efficiency by 5.9%. At an increased solar radiation level from 500 W/m2 to 1000 W/m2, the electrical efficiency of the PVT configuration decreases from 13.75% to 11.1%, while the electrical efficiency of the PVT-PCM configuration falls from 14% to 12% which are 19.3% and 14.3% decreases respectively. These findings clearly showed that, the use of PCM in PVT systems can lead to significant improvements in energy production and cooling processes.

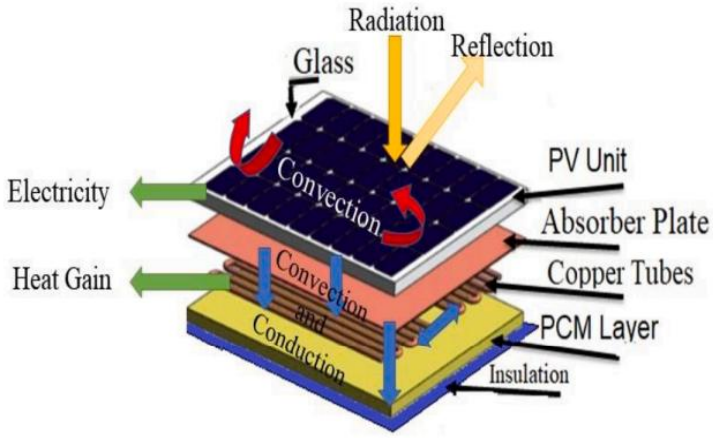


Figure. I.19 *Configuration of the PVT-PCM module showing heat transfer modes.* ***[34]***

Similar to the previously discussed techniques, incorporating porous media into PVT systems significantly increases the heat transfer surface area. This leads to lower cell operating temperatures and more efficient heat dissipation, resulting in an overall improvement in system efficiency.

A study to test the impact of porous media was carried out by **Boulhidja et al. [35]** in **2024**. They conducted a numerical study to investigate the impact of natural convection, the inclination angle (α) of the panel, porous layer thickness (Ep), and the Darcy (Da) and Richard (Ri) numbers, utilizing a porous layer attached to the back wall of the PV module. The calculations were performed using the finite volume method, and a SIMPLE algorithm was applied to effectively manage the pressure–velocity coupling. The results revealed that the electrical and thermal efficiencies of the system improved by up to 9.88% and 10%, respectively, when natural convection was dominant (Ri = 10) at an inclination angle of 45°. Furthermore, a porous layer with moderate permeability (Da = 10^{-3}) could enhance both electrical and thermal efficiencies by more than 23% and 28%, respectively, surpassing traditional PVT systems under specified conditions.

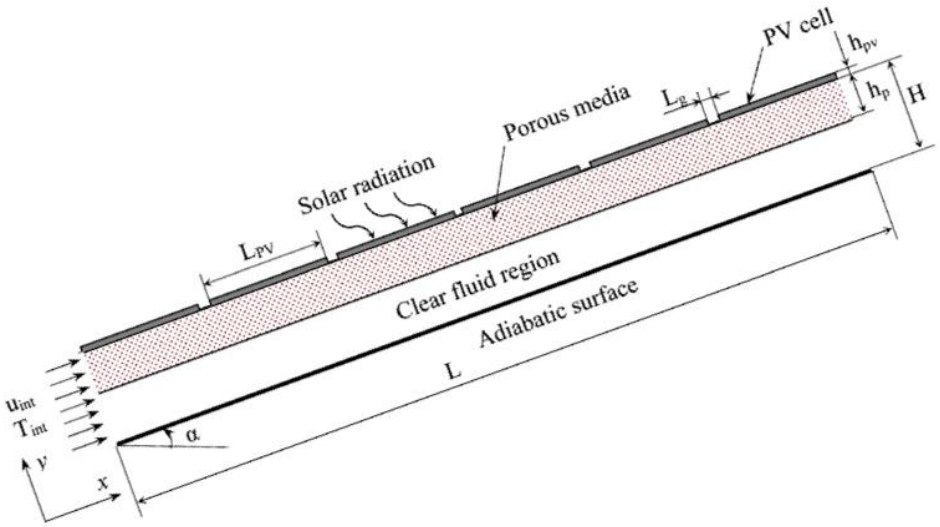


Figure I.20 *Schematic diagram of the PVT integrated with a porous medium* ***[35]***

To achieve more performing systems, multiple cooling techniques can be applied within a single setup. Four distinct systems were established: PV, PVT, PVT-PCM, and PVT-PCM-Porous units. **Rad et al. [36]**. The phase change material used was salt hydrate, while the porous medium consisted of waste industrial aluminium shavings. This study aimed to compare the electrical, thermal, and exergy efficiency of these systems against a standalone

PV unit. The findings from the study, conducted in two different months, July and December, warm and cold revealed that, the PVT-PCM-Porous system exhibited the lowest temperature for the PV cells and the highest electrical power output in both months. A 36.5% reduction in cell temperature and a 17.7% increase in electrical efficiency were noted in July, while in December, the improvements were 33.2% and 14.2%, respectively, compared to the standalone PV unit. Moreover, in July, the addition of aluminium shavings to the PCM resulted in a 6.07% decrease in average thermal efficiency, while the average electrical efficiency increased by 1.43% compared to the PVT-PCM system. In conclusion, these findings demonstrate that the system combination is well-suited for high-temperature applications requiring efficient heat evacuation.

From the above literature review, various techniques have been employed to enhance PVT system performance, each offering unique advantages. These include the addition of a glass cover, incorporation of porous media within the flow passage, utilization of phase-change materials, and the use of nanofluids. These methods either improve the system's protection and/or enhance its electrical and thermal performance primarily through improved PV cell cooling and efficient heat removal. While electrical and thermal efficiencies have greatly improved, further optimization remains possible. This study explores a novel approach, “Optimization of the performance of a thermal photovoltaic solar panel by reducing the flow passage section” an area of research currently unexplored.

CHAPTER II

THEORETICAL STUDY AND MATHEMATICAL FORMULATION

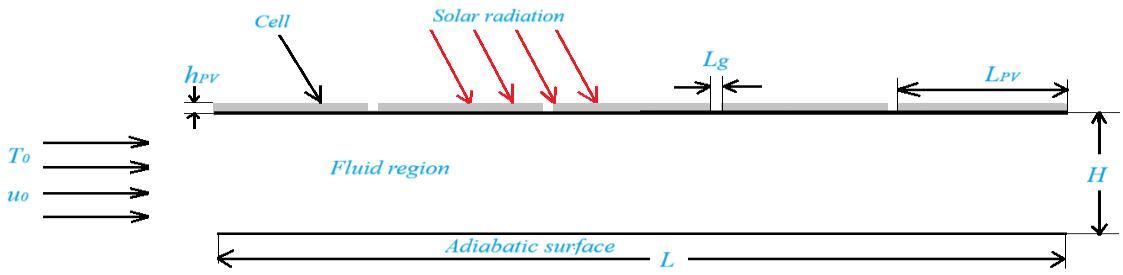
Chapter II

II.1 Introduction

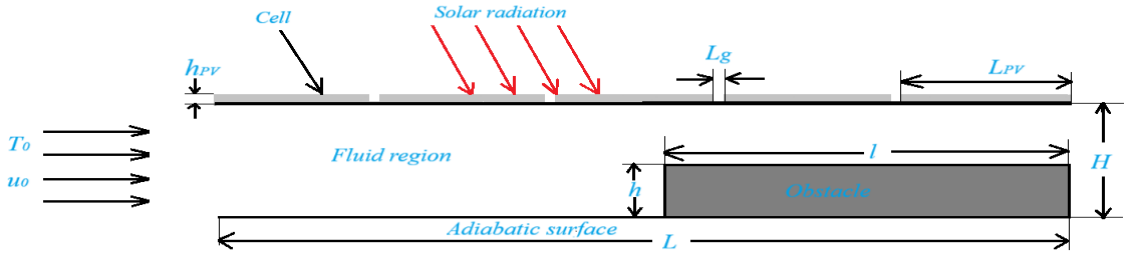
This chapter presents a numerical analysis of two horizontal air-based solar PVT panels without a glass cover. Air is pumped into the channels of the PVT systems to cool the cells by evacuating heat which is used for heating applications. **Figures II.1** below depicts the general structures and key components of the PVT modules. To simplify the analysis, initial and boundary conditions are defined, along with necessary assumptions. Furthermore, the equations governing the resolution of this problem are detailed within this chapter.

II.2 Geometry and Mathematical Model

The studied PVT solar collectors are of, length L and channel height H. Five photovoltaic cells of length L_{PV} and height h_{PV} with a uniform cell to cell separation of L_g are installed on the upper surfaces of the channels where they are exposed to a constant heat flux. The lower wall of the channel is thermally insulated. At the entrance of the channel, the flow enters with an imposed cooler temperature, T_0 and a constant velocity u_0. The coolant absorbs heat continuously throughout its passage to the exit. Two configurations are chosen, the first one is a traditional PVT panel (without a solid layer) which represent the base case (see **Figure II.1a**). In the second configuration, a polypropylene solid layer of variable dimensions, length ***l*** and height *h*, is attached on the bottom wall of the channel directly beneath the last cells which are relatively hotter, **Figure II.1b**.



(a). *Schematic of the traditional PVT collector.*



(b) *Schematic of the modified PVT collector.*

Figure II.1. *Schematic of the studied PVT collector*

II.2.1 Specifications of the studied PVT collectors

The specifications and thermal properties of the studied PVT collector are provided in table **II.1** and **II.2** respectively.

Table II.1. Specifications of the studied PVT

Photovoltaic Thermal Panel (PV)	L_{PV}	185 mm
	L_g	18.75 mm
	h_{pv}	4 mm
	η_{ref}	15%
	β_0	0.0045 k^{-1}
canal	L	1000 mm
	H	50 mm

Table II.2. Thermal Properties of the studied PVT module.

Properties	ρ ($kg.m^{-3}$)	Cp ($J.kg^{-1}.K^{-1}$)	k ($W.m^{-1}.K^{-1}$)	μ ($kg.m.s^{-1}$)
PV Cell	2330	700	148.4	-
Air	1.125	1006.4	0.0242	1.78 X 10^{-5}
Polypropylene	900	1700	0.3	0.28

II.2.2 Simplification Assumptions:

Thermal and physical properties of the different components and the working fluid might vary, but in order to facilitate the mathematical formulations, the following main assumptions are made:

- The fluid flow is considered laminar, steady-state, incompressible and Newtonian.
- Solar radiation is considered to be constant and perpendicular to the photovoltaic panel.
- The obstacle is a perfect rectangle and rigid.
- The bottom surface of the channel is considered adiabatic (isolated)

Table II.3. Dimensional thermal and dynamic boundary conditions

Boundary	Type	Amount
Top	Constant heat flux, no-slip velocity	400 - 1100 W/m^2, v = u = 0
Bottom	Adiabatic wall, no-slip velocity	$\frac{\partial T}{\partial y} = 0$, v = u = 0
Left	Constant temperature, uniform velocity inlet	T_0 = 298K, Re = 500 - 2000
Right	Thermal and dynamic establishment	v = 0, $\frac{\partial u}{\partial x} = 0, \frac{\partial T}{\partial x} = 0$

II.2.3 Mathematical Formulations

Under the above assumptions, the mathematical model developed to simulate the forced convection in the entire channel is as follows (Navier-Stokes equations):

Continuity equation:

$$\frac{\partial \mathrm{u}}{\partial \mathrm{x}} + \frac{\partial \mathrm{v}}{\partial \mathrm{y}} = 0 \qquad (\mathbf{II.\,1})$$

x—component of momentum equation:

$$\left(\mathrm{u}\frac{\partial \mathrm{u}}{\partial x} + v\frac{\partial \mathrm{u}}{\partial y}\right) = -\frac{1}{\rho_0}\frac{\partial p}{\partial x} + \nu\left(\frac{\partial^2 \mathrm{u}}{\partial x^2} + \frac{\partial^2 \mathrm{u}}{\partial y^2}\right) \qquad (\mathbf{II.\,2})$$

y—component of momentum equation:

$$\left(\mathrm{u}\frac{\partial \mathrm{v}}{\partial x} + \mathrm{v}\frac{\partial \mathrm{v}}{\partial y}\right) = -\frac{1}{\rho_0}\frac{\partial p}{\partial y} + \nu\left(\frac{\partial^2 \mathrm{v}}{\partial x^2} + \frac{\partial^2 \mathrm{v}}{\partial y^2}\right) \qquad (\mathbf{II.\,3})$$

Energy equation for the channel

$$\left(\mathrm{u}\frac{\partial T}{\partial x} + \mathrm{v}\frac{\partial T}{\partial y}\right) = \frac{k}{\rho Cp}\left(\frac{\partial^2 T}{\partial x^2} + \frac{\partial^2 T}{\partial y^2}\right) \qquad (\mathbf{II.\,4})$$

Energy equation for the PV cells and obstacle:

$$\frac{\partial^2 T}{\partial x^2}+\frac{\partial^2 T}{\partial y^2}=0 \qquad (\mathbf{II.5})$$

where ρ, ν et k represent the density, kinematic viscosity and thermal conductivity of the fluid respectively. In addition, we used the following dimensionless variables (Eq. 7) to write the previous equations in dimensionless form

$$(X,Y)=\frac{(x,y)}{H},\theta=\frac{k_f(T-T_0)}{QH}\ ,\quad P=\frac{p}{\rho u_0^2}\ ,(U,V)=\frac{(\mathrm{u,v})}{u_0} \qquad (\mathbf{II.6})$$

So, the dimensionless equations are:

Continuity equation:

$$\frac{\partial U}{\partial X}+\frac{\partial V}{\partial Y}=0 \qquad (\mathbf{II.7})$$

Momentum equations

$$\left(U\frac{\partial U}{\partial X}+v\frac{\partial U}{\partial Y}\right)=-\frac{\partial P}{\partial X}+\frac{1}{Re}\left(\frac{\partial^2 U}{\partial^2 X}+\frac{\partial^2 U}{\partial^2 Y}\right) \qquad (\mathbf{II.8})$$

$$\left(U\frac{\partial V}{\partial X}+v\frac{\partial V}{\partial Y}\right)=-\frac{\partial P}{\partial Y}+\frac{1}{Re}\left(\frac{\partial^2 V}{\partial^2 X}+\frac{\partial^2 V}{\partial^2 Y}\right) \qquad (\mathbf{II.9})$$

Energy equation for the channel

$$\left(U\frac{\partial \theta}{\partial X}+V\frac{\partial \theta}{\partial Y}\right)=\frac{1}{PrRe}\left(\frac{\partial^2 \theta}{\partial X^2}+\frac{\partial^2 \theta}{\partial Y^2}\right) \qquad (\mathbf{II.10})$$

Energy equation for the PV cells and obstacle:

$$0=\frac{\partial^2 \theta}{\partial X^2}+\frac{\partial^2 \theta}{\partial Y^2} \qquad (\mathbf{II.11})$$

Where Pr = $\frac{\mu.Cp}{\lambda}$ and Re = $\frac{\rho.H.u_0}{\mu}$

where μ is the dynamic viscosity and λ is the thermal conductivity.

II.3 Efficiencies of the PVT system [40,44].

Moreover, the performance of the air-based PVT system can be evaluated based on the expressions of thermal, electrical and overall efficiencies.

II.3.1 Thermal Efficiency

Thermal efficiency of the PVT system, η_{Th}, defines the amount of heat energy produced by the PVT system from the absorbed solar irradiance. $\eta_{Th}$is modelled by:

$$\eta_{\mathrm{Th}} = \frac{\mathrm{Q_u}}{\phi \cdot \mathrm{A_c}} \qquad (\mathbf{II.12})$$

where A_c is the collector surface area, ϕ signifies the solar irradiation per unit area and Q_u is the useful thermal energy transferred to the working fluid, which could be expressed as follows:

$$\mathrm{Q_u} = \dot{\mathrm{m}} \times \mathrm{Cp} \times (\mathrm{T_{out}} - \mathrm{T_0}) \qquad (\mathbf{II.13})$$

With $\dot{m}$, Cp, T_{out}, and T_0 being the mass flow rate, specific heat, and the average outlet and inlet temperatures of the fluid respectively.

The average fluid outlet temperature is calculated by the following relationship:

$$\mathrm{T_{out}} = \int_0^{\mathrm{H}} \mathrm{u \cdot T \cdot dy} \Big/ \int_0^{\mathrm{H}} \mathrm{u \cdot dy} \qquad (\mathbf{II.14})$$

II.3.2 Electrical Efficiency

The electrical efficiency of a PVT system, η_{El}, is a measure of how effectively the PV cells convert incoming solar radiation into electrical power. This efficiency is calculated using the following equation:

$$\eta_{\mathrm{El}} = \eta_{\mathrm{Ref}} \times \left(1 - \beta_0 \times (\mathrm{T_{PV}} - 298)\right) \qquad (\mathbf{II.15})$$

where η_{Ref} is the electrical yield of the PV panel under reference conditions and β_0 represents the thermal expansion coefficient (as given in table II.1), while T_{PV} is the average temperature of the photovoltaic panel. The average PV cells temperature is given by the following formula:

$$\mathrm{T_{PV}} = \int_0^{\mathrm{L}} \mathrm{T \cdot dx} \qquad (\mathbf{II.16})$$

II.3.3 Overall Efficiency

The overall efficiency, also known as the total efficiency (η_{Tot}) of a PVT system quantifies its effectiveness in converting solar radiation into useful energy. It is defined as the ratio of the total useful energy output to the incident solar radiation. This overall efficiency is determined by summing the electrical and thermal efficiencies, as detailed in Equation II.7.

$$\eta_{Tot} = \eta_{El} + \eta_{Th} \qquad \text{II. 7}$$

II.4 Numerical processing and mesh effect

In this study, the 2D Navier-Stokes equations are used to describe the air flow in the channel. A FORTRAN computer code which was developed based on the Finite Volume Method (FVM) is used to solve the equations of momentum, energy, and continuity, while the Semi Implicit Method for Pressure Linked-Equations (SIMPLE) algorithm is used to address the pressure-velocity coupling. The results from this simulation are interpreted in form of graphs using the ORIGIN software while the temperature and velocity contours are drawn using TECPLOT.

II.4.1 The simple algorithm

The SIMPLE algorithm solves the discretized equations iteratively. This algorithm stipulates the existence of a relationship between the corrected velocities and the corrected pressures in order to verify the mass conservation equation. It links corrected velocities and pressures to ensure mass conservation. Initially, a fixed random initial pressure field is used in the momentum equation to calculate a preliminary velocity field. The mass and momentum equations are then used to correct these initial pressure and velocity fields. Other transport equations are solved, and the corrected pressure field initializes the next iteration. This iterative process continues until convergence criteria is met.

II.4.2 Convergence criteria (Residual)

An iterative procedure is convergent if all errors tend to decrease during the iterations i.e., when iterations produce minor changes in the variables according to the user's convergence criteria. The convergence criterion used in our calculation program is based on the residuals of the equations of the problem. The residual corresponds to the sum, over all the mesh points,

of the errors made on the discretized equation in question when the variables determined by the process are reintegrated into the discretized equation.

By definition:

$$R = \sum_{mesh} \left(\sum_{nb} \left(a_{nb} \emptyset + S_{\emptyset} - a_p \emptyset_p \right) \right) \qquad (\mathbf{II.17})$$

For the pressure equation, the corresponding residual concerns the conservation of mass. Its value is given by the following relation:

$$R = \sum_{node\ P} |(\rho u A)_e - (\rho u A)_w + (\rho u A)_n - (\rho u A)_s| \qquad (\mathbf{II.18})$$

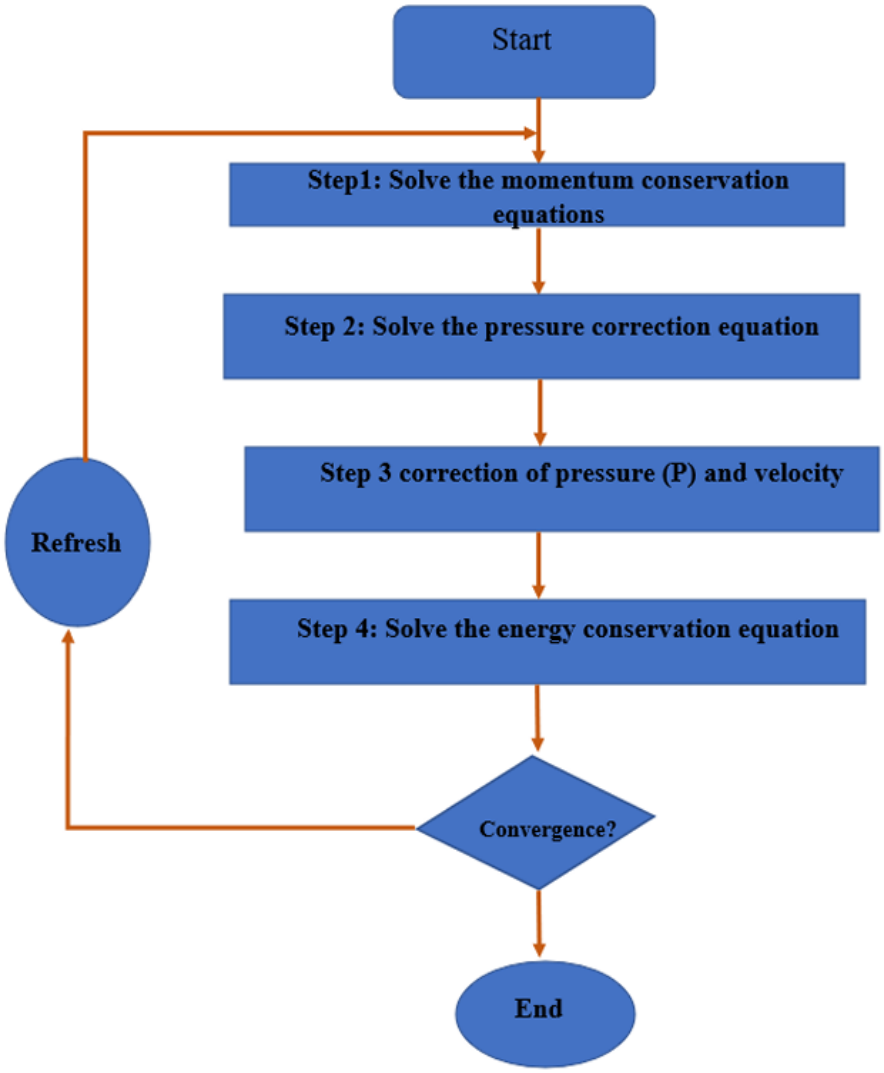


Figure II.2 *Representative organigram of the SIMPLE algorithm* ***[45]***

II.4.3 The mesh effect

For the solver's results to be accurate and reliable, they must not depend on the mesh density, the solution should be independent of the grid size used. To verify this, we monitor the change in a key variable, like the electrical efficiency, as we progressively refine the mesh. In this case, the independence between the numerical results and the mesh is verified for different grid sizes (3600, 6800, 9900, 13600, 18000 and 23000). **Figure II.3** shows the effect of grid sizes on the electrical and thermal efficiencies of the PV cells for Re=1000, Pr = 0.71, l=0.5L and h=0.5. It is clear from this figure that, for grid sizes above 18000, no significant variation in the numerical data is observed. Therefore, a grid size of 18000 (60×300) is preferred for studying this problem.

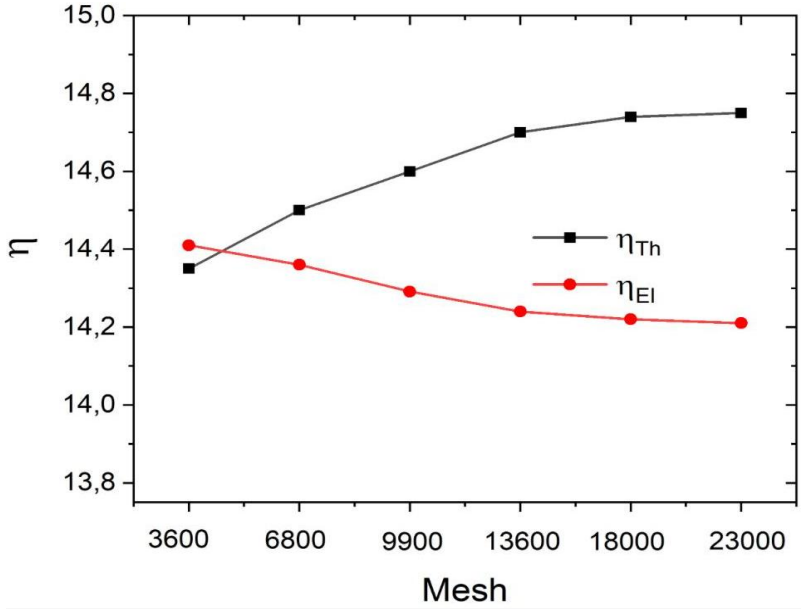


Figure II.3. *Meshing effect on the average outlet and average PV cells temperatures*

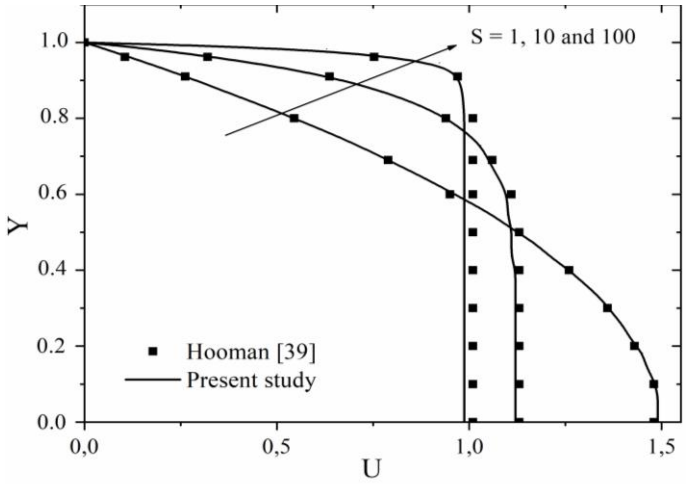
II.4.4 Code validation

To validate the calculation code, two different tests are proposed. The first validation is carried out with the numerical results of **Hooman et al. [39]** for the case of forced convection in a porous channel. As shown in figure II.3, an excellent agreement is observed between our numerical results (velocity U) and those presented by Hooman et al. for different values of the Darcy number. The second validation is obtained by comparing the numerical asymptotic values of the Nusselt number with the corresponding analytical values and numerical values of **Radwan et al. [40]** for different heating positions (see figure II.4 and table II.3).

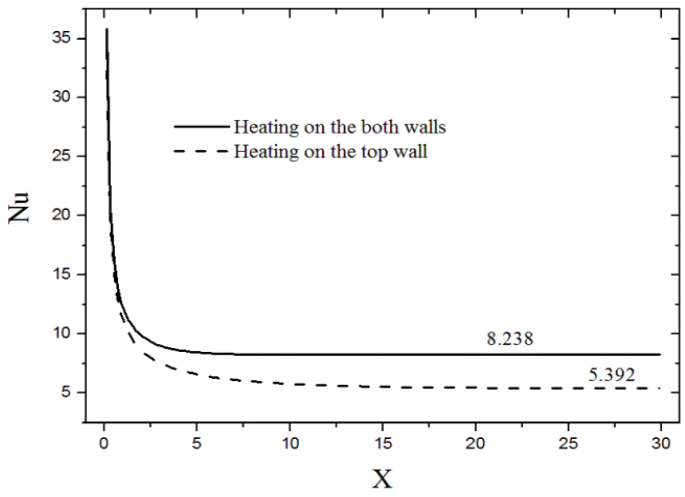
It can be seen in Figures II.3-4 and Table II.4 that, the numerical accuracy of the calculation code is verified to carry out this study.

Table II.4. *Validation of the asymptotic values of the Nusselt number*

	Analytical values	Radwan et al.	Present
Both wall	8.235	8.28	8.238
One wall	5.385	5.42	5.392



(a) *Validation of the U-velocity profiles with those of Hooman, as a function of S* ***[39]*** *(*$S = 1/\sqrt{Da}$*)*



(b) *Validation of Nusselt number with the one of Radwan et al.* ***[40]*** *for different heating position*

Figure II.4 Validation of code.

Chapter III

Results and Discussion

Chapter III

III.1 Introduction

This chapter presents the results obtained during the numerical simulation together with the observations and discussions made. This study focuses on optimizing PVT panel performance by utilizing a solid layer, described in **Chapter II**, **Figure. II.1**. The first part concentrates on the classical PVT collector (without solid layer) where the effect of Reynolds number and incident radiation is examined. In the second case, a solid layer is inserted on the bottom wall of the channel under the last cells. In this case the influence of the height and length of the solid layer are analysed. The results of this study are presented in terms of dynamic and thermal fields, average cell and outlet temperatures as well as thermal and electrical efficiencies.

III.2 Case 1: Classical PVT collector

This section examines how different Reynolds numbers ($500 \leq Re \leq 2000$) and daytime, influence the overall performance of the PVT system. Indeed, the best results of this case (without a solid layer) are used as a reference case for comparison.

Figure III.1 presents the average amount of radiation received in W/m² in the wilaya of Biskra, Algeria across three different seasons, summer, spring and winter, from 07:00 to 18:00. The quantity of solar radiation reaching Earth is influenced by both the time of year and the time of day. On a daily basis, the received radiation increases from morning, peaks at midday, and then decreases towards sunset, creating a parabolic distribution. Summer months generally receive abundant solar radiation, while winter months receive less. Consequently, this study investigates the cooling of a PVT solar panel during the summer season. The values of average diurnal solar radiation for the summer period, as derived from Figure III.1, are presented in **Table III.1**.

***Table III.1**. Average solar radiation levels throughout daylight hours in summer.*

Time	08:00	09:00	10:00	11:00	12:00	13:00	14:00	15:00	16:00	17:00
Radiation Q(W/m²)	400	650	830	1000	1100	1100	1000	900	650	450

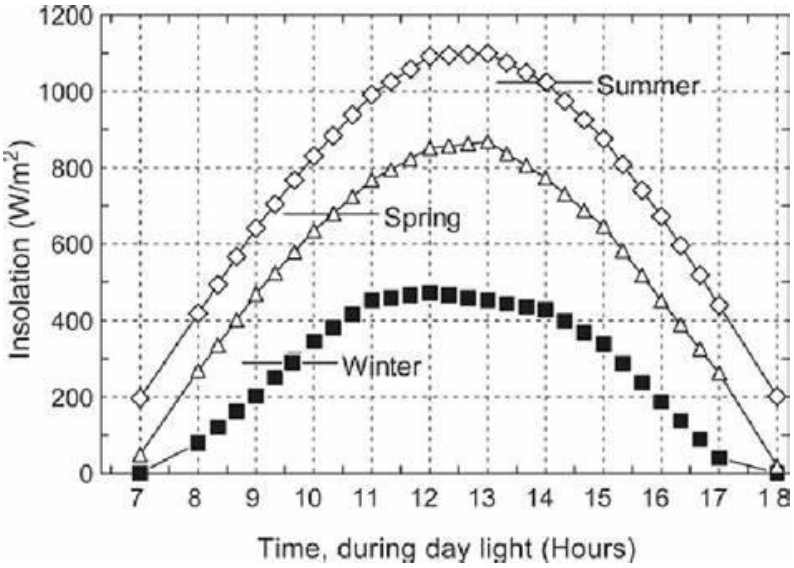
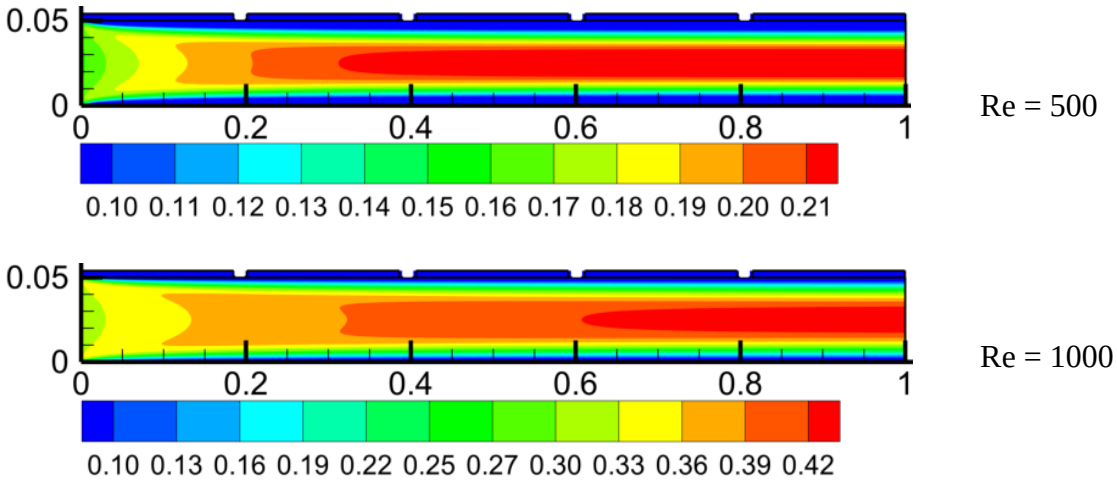
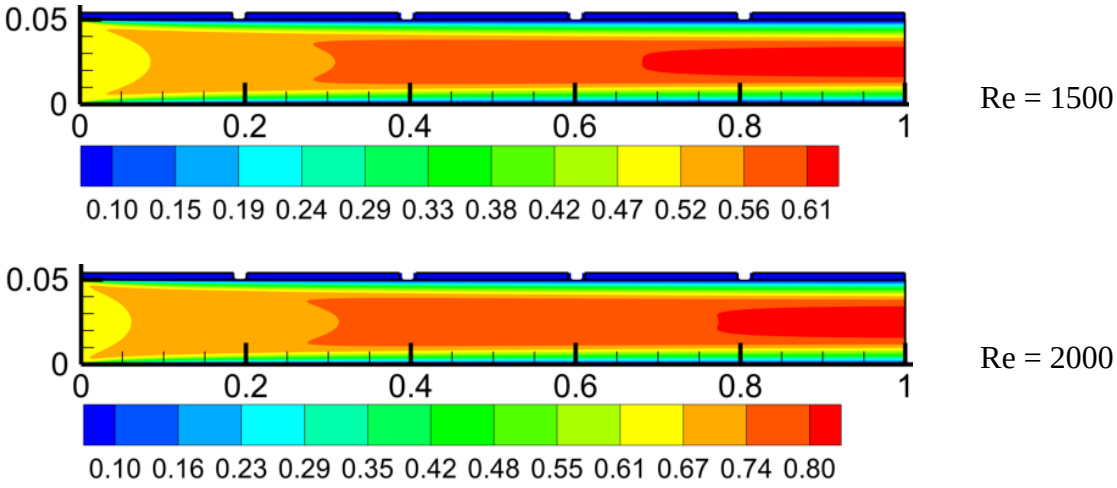


Figure III.1. *Solar radiation levels throughout the day in summer, winter, and spring.**[41]***

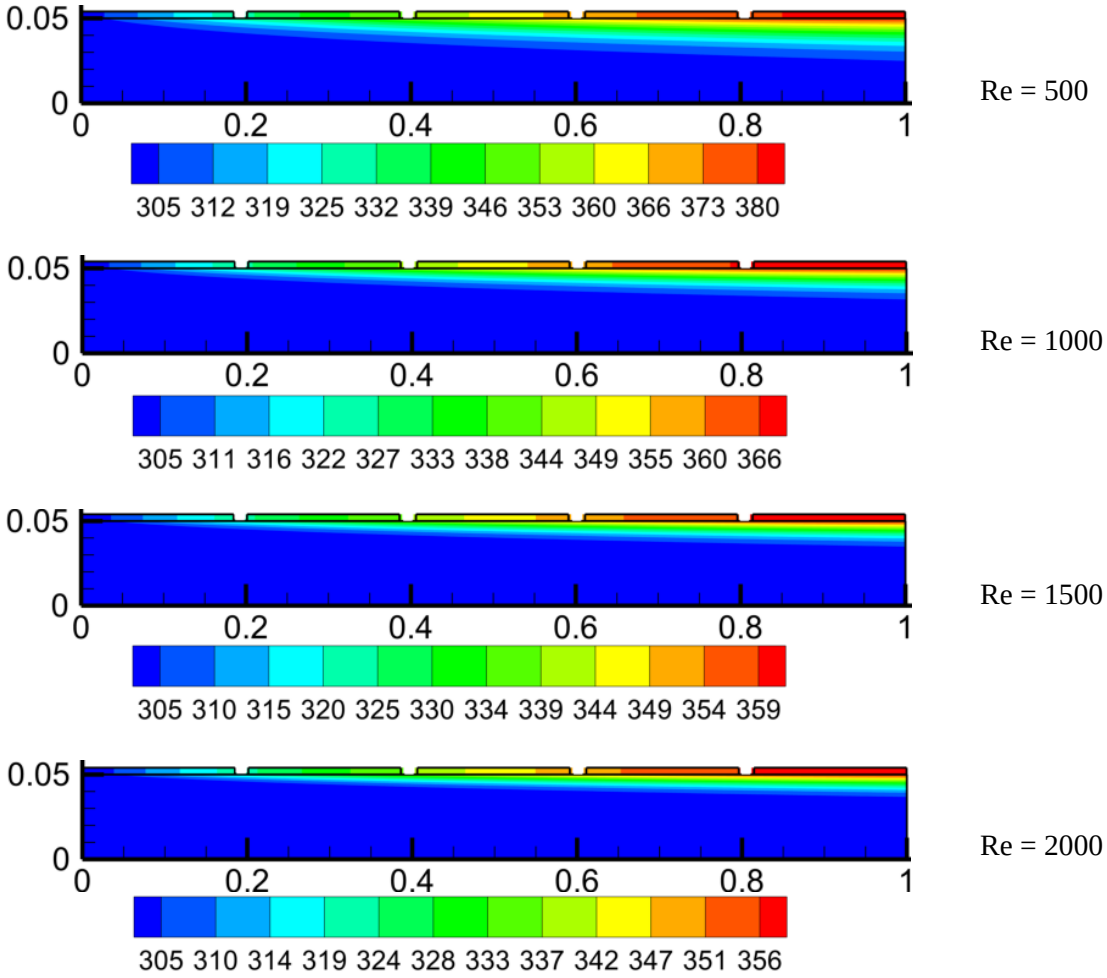
Figure III.2a illustrates the impact of the Reynolds number (Re) on the velocity distribution within a simple PVT panel (without solid layer) at 11:00 (Q = 1000W/m²). The velocity contours remain symmetrical across the channel's midpoint (y = H/2) for all tested Re values. As Re increases from 500 to 2000, the airflow strengthens, indicated by rising fluid velocities, from approximately 0.21 m/s to 0.80 m/s.

For the thermal fields, **figure III.2b**, a consistent cell temperature increase towards the exit of the flow passage is noticed across all Re numbers. This is because the fluid enters cold, absorbing heat from the cells, thus cooling the cells less effectively at the exit compared to the entrance. Furthermore, the maximum cell temperature (at the panel exit) decreases from 380K to 356K as the Re number rises. This reduction is a result of improved convective effect, as the faster-moving fluid more effectively removes heat from the system.





(a) *velocity contours.*



(b) *Isotherms.*

Figure III.2 (a) velocity contours and (b) thermal fields for different values of Reynolds number (Re = 500 to 2000) and solar radiation (ϕ = 1000W/m^2).

The effect of the daytime for different Reynolds number on the average PV cells temperature (T_{PV}) and the average fluid outlet temperature (T_{Out}), are presented in **Figure III.3** and **Figure III.4** respectively. As depicted in these figures, it can be seen that T_{PV} and T_{Out} decrease with the increase in the Re number. The decrease in T_{PV} is attributed to the enhanced cooling due to the increase of the convective effect while the decrease in the T_{Out} is due to the fact that the coolant spends less time within the channel at higher flow velocities. The increase in daytime leads to an increase in both average temperatures up to 12:00 followed by a decrease towards 17:00 forming a parabolic variation for all the studied Re numbers. In addition, it is important to note that the increase rate of both average temperatures with time decreases with increasing Re.

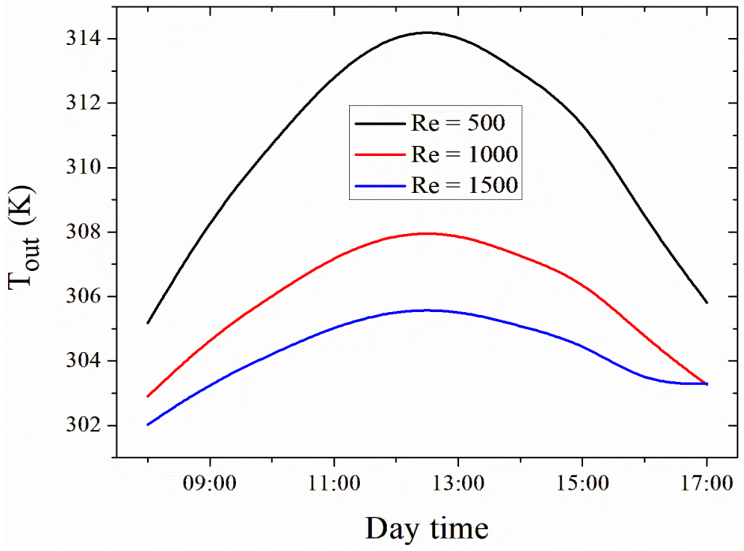


Figure III.3. Daytime influence *on average outlet temperature at different Re number.*

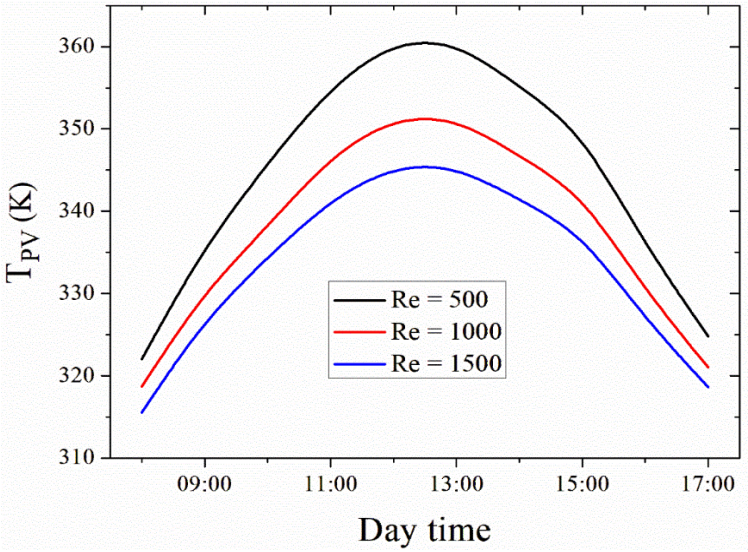


Figure III.4. Daytime influence *on the PV cells' temperature at different Re number.*

The impact of Reynolds number, Re, and daytime on the thermal (η_{Th}) and electrical (η_{El}) efficiencies of the PVT system are illustrated in **Figure III.5**. and **Figure III.6** respectively. From figure 3.5, the η_{El} presents an inverse trend compared with the average PV cells temperature which are linked by the equation II.15. In fact, it peaks at the beginning and end of the day (08:00 and17:00) and reaches its lowest point during the afternoon (12:00-13:00). By increasing Re number, an enhancement in the η_{El} of around 9.3% is noticed. Shifting our attention to the η_{Th}, it is observed that η_{Th} remains consistent throughout the daytime irrespective of Re numbers. The reason for this is the constant nature of the ratio $(T_{out} - T_{in})/\phi$, which is the core of the thermal efficiency calculation, as expressed in equation II.12. On the other hand, the thermal efficiency increases by about 17.86% when Re number increases from 500 to 1500 due to a more significant rise in the mass flow rate over the drop in the average outlet temperature.

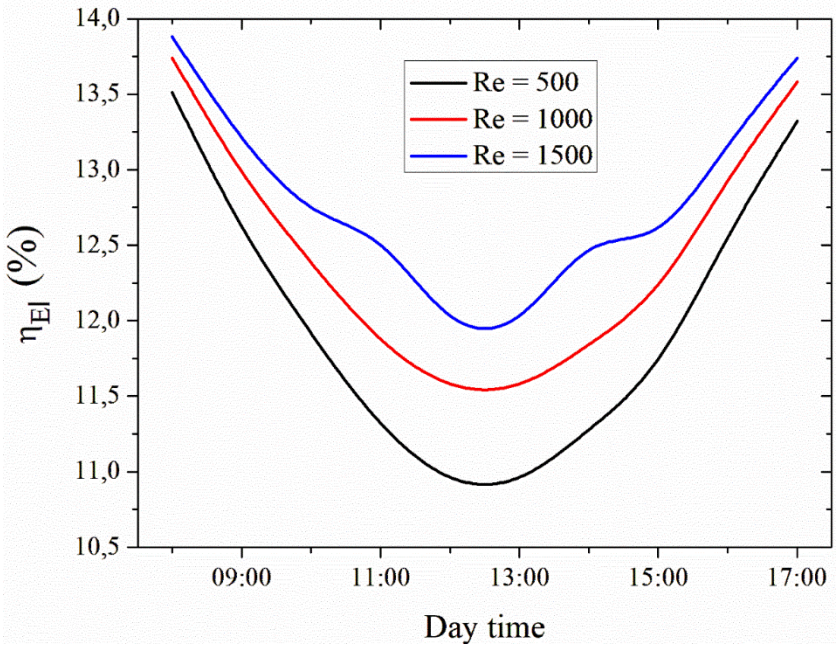


Figure III.5. Daytime influence *on the panel's electrical efficiency at different Re number.*

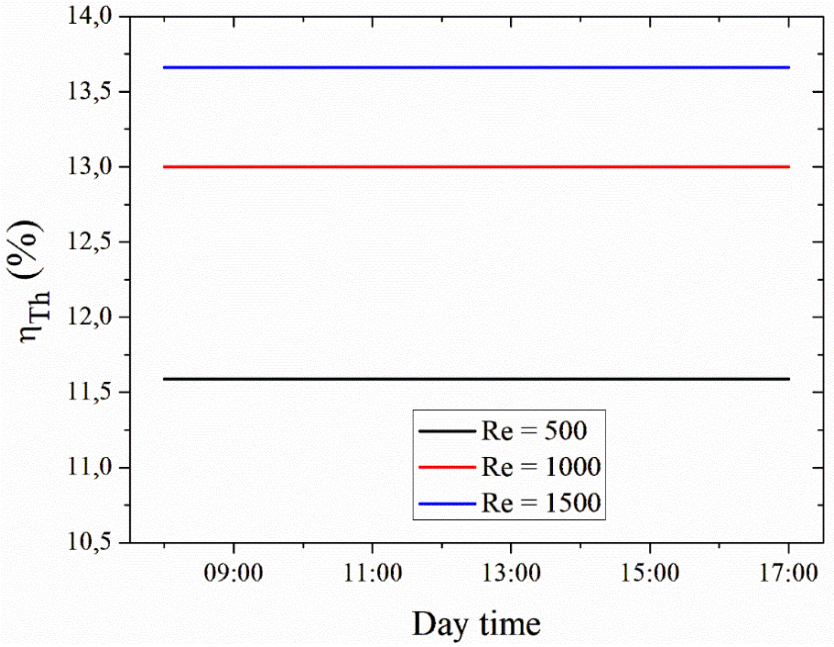


Figure III.6. *The influence of diurnal radiation on the panel's thermal efficiency at different Reynolds number.*

III.3 Case 2: Effect of solid layer insertion

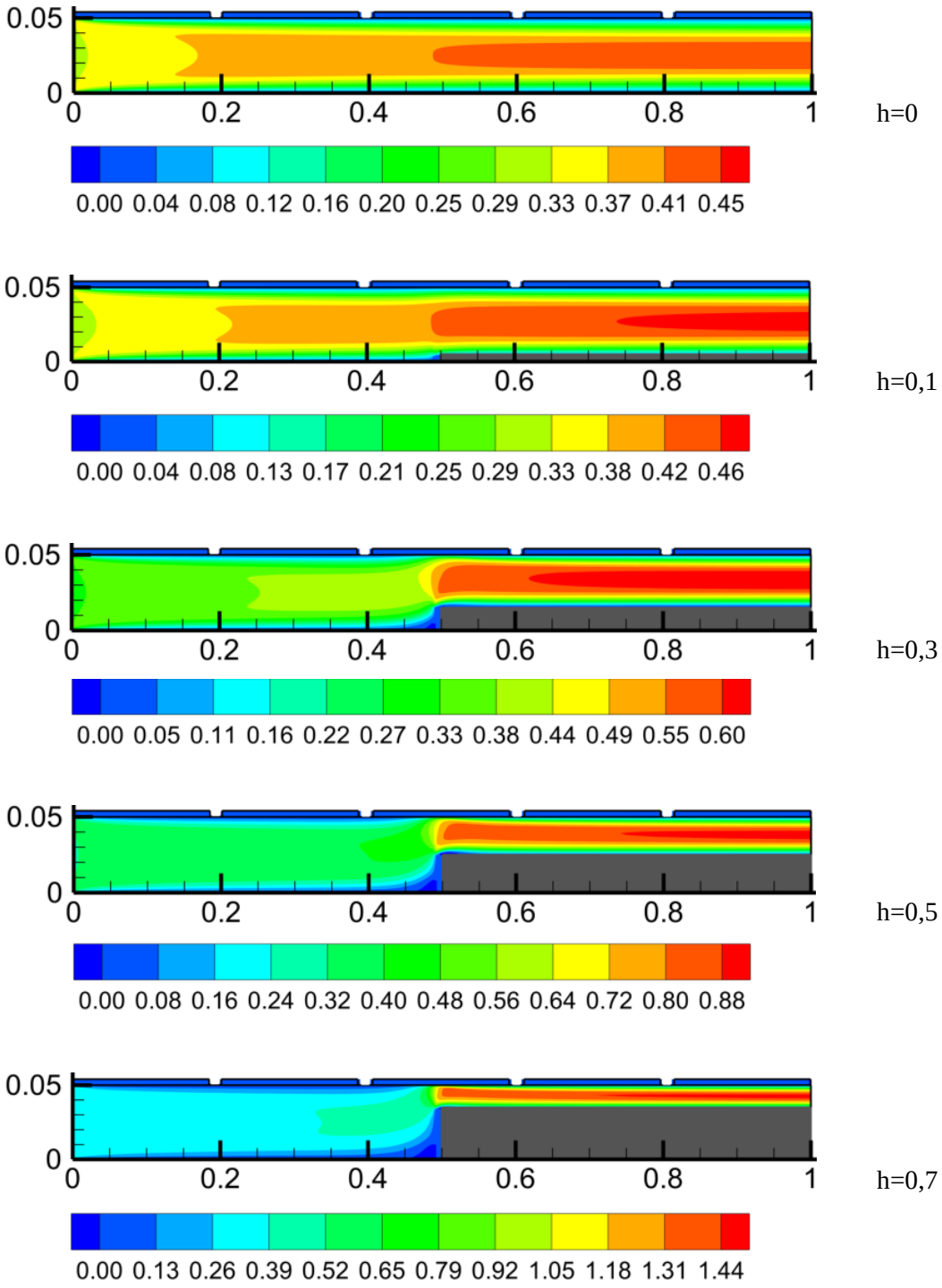
In this section, a solid layer is inserted on the bottom of the channel to decrease flow passage area in order to increase the coolant velocity especially under the last cells which are relatively hotter. The effect of varying the dimensions of the solid layer (length and height) were examined while maintaining Re number at 1000 and radiation at 1000W/m^2.

III.3.1 Effect of Solid layer height

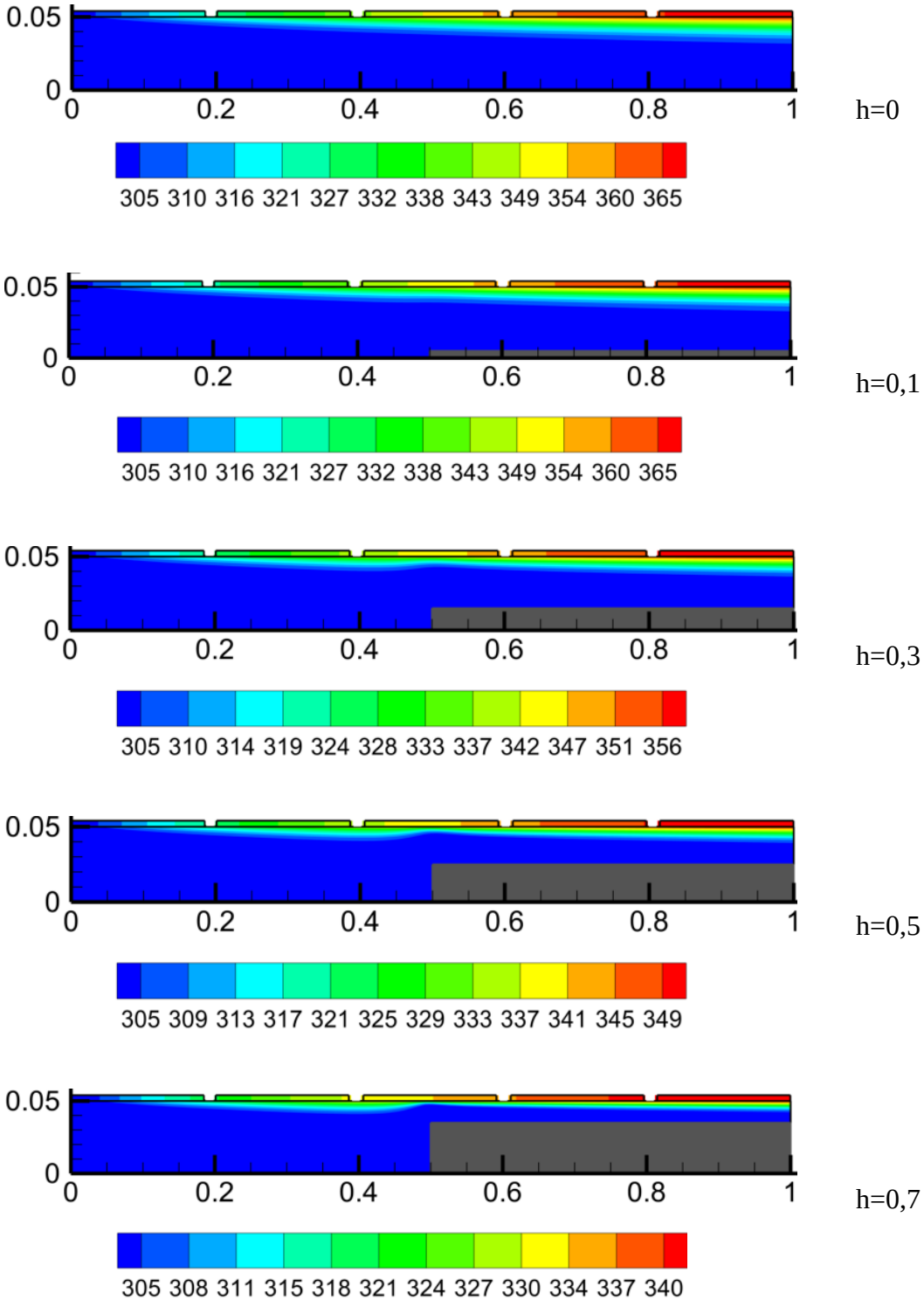
In order to investigate the effect of height (h) of the solid layer, h is varied from 0.1 to 0.7 and compared to h=0 (without solid layer).

Figure 3.7(a) shows the effect of solid layer height on the dynamic fields for the length, l = 0.5 L. The results presented in this figure demonstrate a continuous increase in the fluid velocity towards the outlet for all the values of h. In fact, in the absence of a solid layer, qualitative and quantitative symmetries on the x-velocity are observed. When a solid layer of height h=0,1 is used, the dynamic pattern starts to lose its symmetries. By increasing h beyond 0.1, these symmetries are completely lost and leading to the creation of another distinct channel (dynamic establishment between solid layer and last cells). For elevated height values (h=0,7), the coolant shows increased velocity, resulting in jet-like flow reaching a maximum velocity of 1.44m/s, which can be observed from the air velocity profile at the outlet of the panel as presented in **Figure III.7a**.

The evolution of thermal field of the system on varying the height of the solid layer are shown in **Figure III.7(b)**. It is observed from this figure that due to the unchanged fluid flow intensity when a solid layer of h =0.1 is inserted, the thermal field remains similar to the case without a solid layer. By increasing h beyond 0.1, the maximum temperature of the system decreases significantly due to the increase in the convective effect (it decreases from 365 for h=0.1 to 340 for h=0.7.



(a) *Velocity contours.*



(b) *Isotherms.*

Figure III.7 (a) velocity contours and (b) thermal fields as a function of solid layer height (h = 0 to 0.7) for Re = 1000 and solar radiation (ϕ = 1000W/m^2).

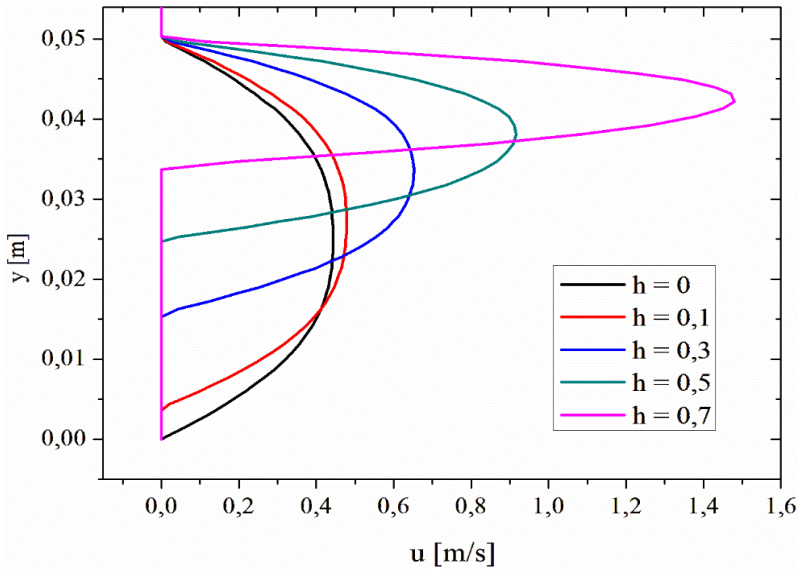
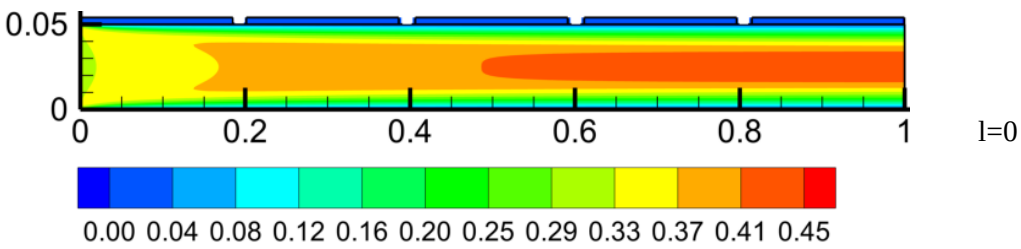


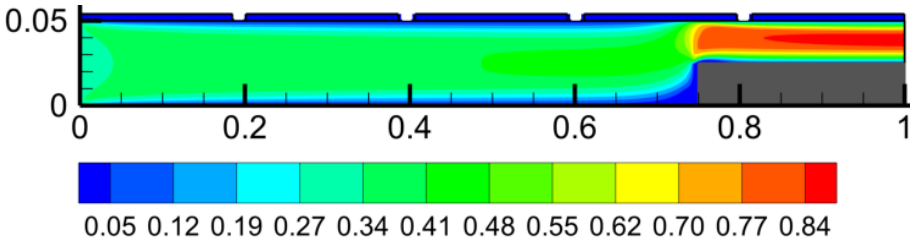
Figure III.8. *Velocity profile for different values of h.*

III.3.2 Effect of solid layer length

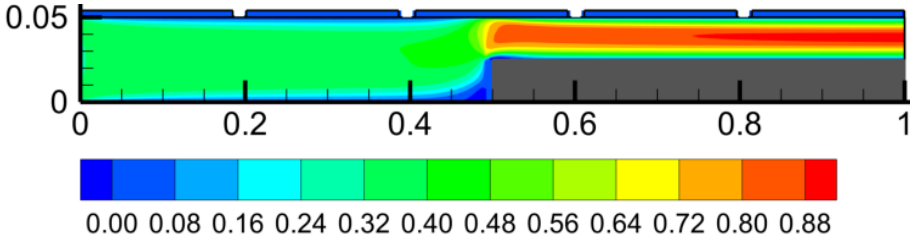
Figures 3.9 illustrates the dynamic and thermal fields of the system, examining the impact of varying the solid layer length, l, while maintaining a fixed height, $h = 0.5L$, a Reynolds number of 1000, and radiation of 1000 W/m². Figure 3.9 (on the upper) reveals a significant increase in the maximum system velocity. Specifically, a substantial increase of approximately 86.67% is observed between the velocity of traditional system (without a solid layer) and that of the system with a solid layer length of $l = 0.25L$. Further increases in the solid layer length beyond $0.25L$ result in only slight changes in maximum velocity, a 4.76% increase from $l = 0.25L$ to $0.5L$, and a 1.13% from $l = 0.5L$ to $0.75L$. This result can be confirmed by **Figure III.10** which illustrates the effect of the solid layer length on the air velocity profile.

The corresponding thermal field (**Figure III.9 on the lower**) highlights a notable maximum temperature drop between the traditional case and the case with $l = 0.25L$. This is attributed to the enhanced airflow resulting from the reduced channel area when the solid layer is introduced. The rate of temperature drop diminishes as the solid layer length increases, remaining essentially constant for $l = 0.5L$ and $0.75L$. Consequently, it is evident that the solid layer of length 0.5L is the optimum length for the material and cost point of view.

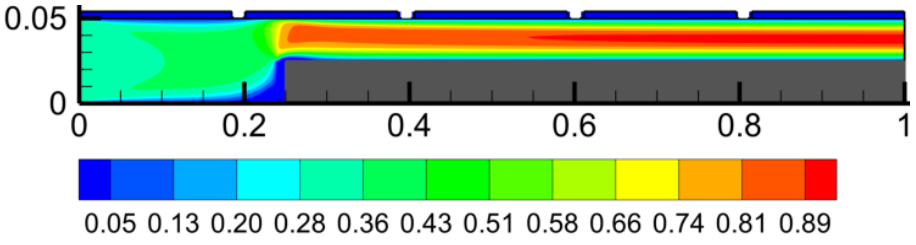




l=0.25L

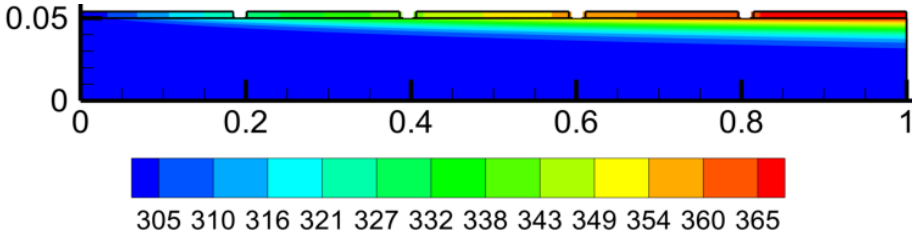


l=0.5L

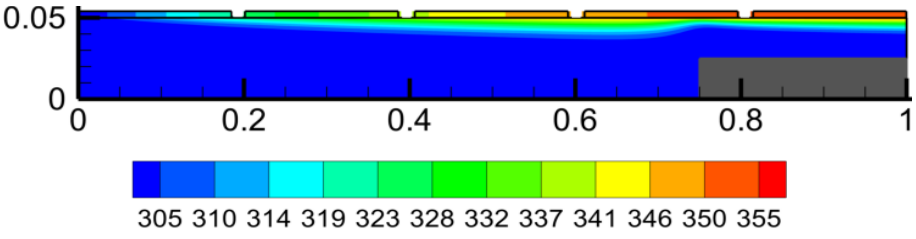


l=0.75L

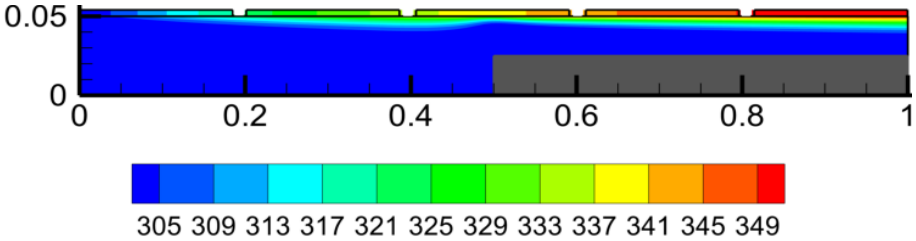
(a) *Velocity contours.*



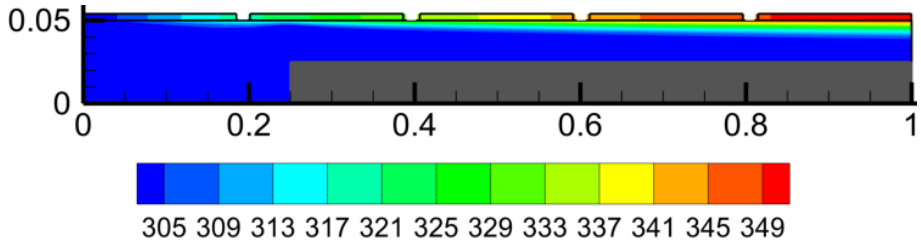
l=0



l=0.25L



l=0.5L



l=0.75L

(b) *Isotherms.*

Figure III.9 (a) velocity contours (b) and thermal fields as a function of solid layer length (l = 0 to 0.75L) for Re = 1000 and solar radiation (ϕ = 1000W/m^2).

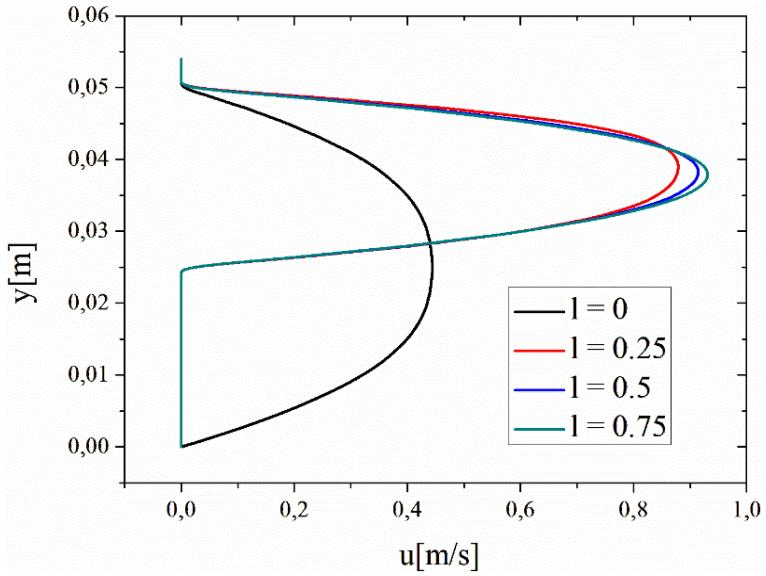


Figure III.10. *Velocity profile for different values of l.*

A graphical representation of the effect of varying the solid layer dimensions (height, h and length, l) on the electrical (η_{El}) and thermal (η_{Th}) efficiencies of the PVT system are shown on **Figure III.11** and **Figure III.12** respectively. From Figure III.11, it is observed that for a fixed length of the solid layer, η_{El} increases almost linearly with h. This enhancement is primarily attributed to improved PV cell cooling facilitated by the accelerated coolant flow within the constricted channel. Increasing the length (l) from 0.25L to 0.5L results in a notable electrical efficiency gain of approximately 2.6%. However, further increases in length beyond 0.5L have a negligible effect on electrical efficiency, due to the fact that the cells are already effectively cooled at the inlet.

By examining η_{Th}, **Figure III.12**, it is observed that η_{Th} exhibits a positive correlation with increasing solid layer dimensions. Its rate of increase is initially gradual when h is increased

from 0 to 0.45, but becomes more pronounced beyond h = 0.45. Compared to the electrical efficiency, thermal efficiency is more sensitive to changes in solid layer dimensions, achieving a maximum enhancement of 26.15%, across all tested values of h and l.

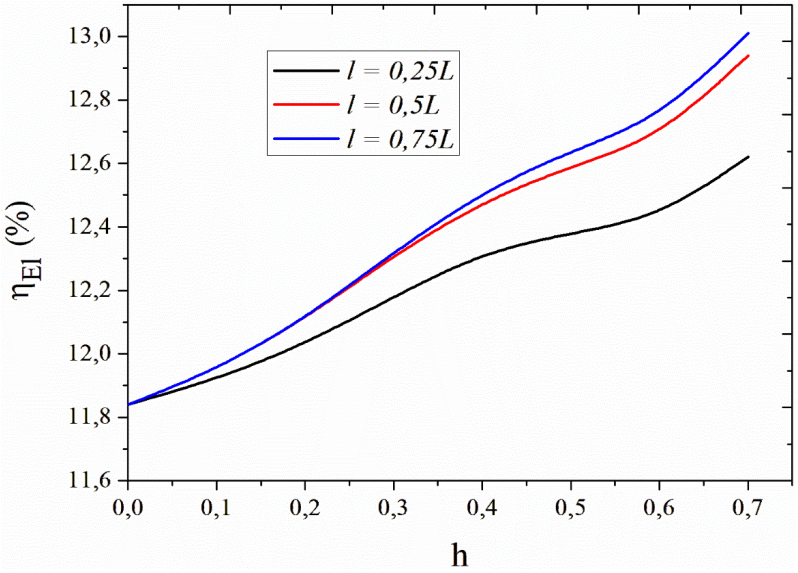


Fig III.11. *Graphical interpretation of the impact of the variation of h and l on the electrical efficiency.*

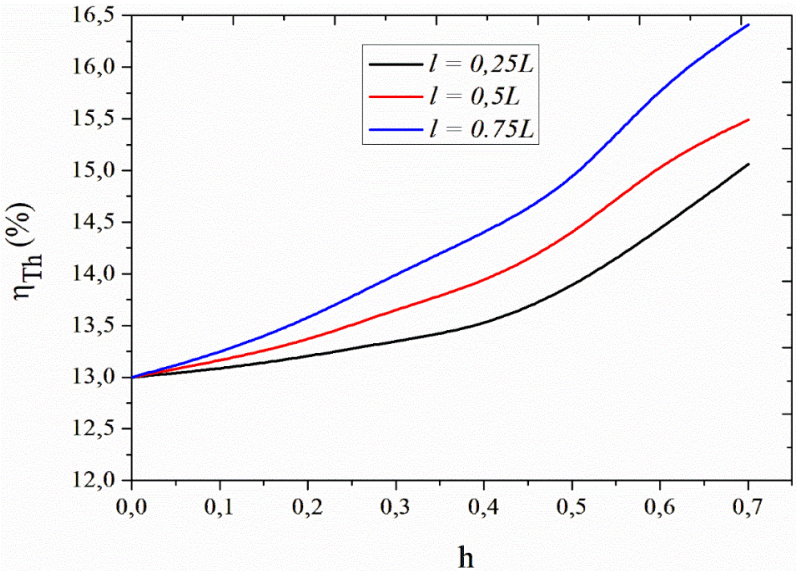


Fig III.12. *Graphical interpretation of the impact of the variation of h and l on the thermal efficiency.*

General Conclusion

General conclusion

In this work, we investigated the optimization of electrical and thermal efficiencies of a PVT collector by reducing the fluid flow area. The governing mathematical formulations are solved using the Finite Volume Method and the SIMPLE algorithm to handle the pressure-velocity coupling. A comparative study was conducted between a conventional PVT collector and a modified design incorporating a solid layer beneath the last cells.

Firstly, we varied the Reynolds number and the daytime in the conventional PVT collector. The results showed remarkable improvements in the electrical and thermal efficiencies of the system. A maximum electrical efficiency gain of 9.17% between 12:00 and 13:00 and a thermal efficiency gain of 17.86% regardless of the daytime were observed when Re was increased from 500 to 1500.

In the second case, a solid layer was inserted on the traditional collector, and the dimensions were varied while maintaining Reynolds number at 1000 and solar irradiance at 1000W/m^2. An increase in the height of the solid layer showed a positive impact on the electrical and thermal efficiencies for all studied values of l. Maximum performance was observed at h = 0.7, achieving maximum improvements of 3.17% and 9.33% in electrical and thermal efficiency, respectively.

Under 1000 W/m² solar radiation and Re = 1000, the modified PVT collector significantly outperformed the conventional design, exhibiting 9.74% and 19.23% improvements in electrical and thermal efficiency, respectively. The optimal solid layer length was determined to be 0.5L, offering a balance between performance and material cost. This passive design modification effectively enhances PVT system performance at lower Reynolds numbers, eliminating the need for external energy input to increase fluid velocity.

References

[1] https://www.un.org/en/climatechange/raising-ambition/renewable-energy#

[2] F. N. Roudbari, H. Ehsani, S. R. Amiri, A. Samadani, S. Shabani, A. Khodadad, “Advances in photovoltaic thermal systems”, A comprehensive review of CPVT and PVT technologies, Solar Energy Materials and Solar Cells, 267, 2024

[3] E. Nehrenheim, “Introduction to Renewable Energies”, Mälardalen University, Västerås, Sweden, 2018, pp 405-406

[4] Zohuri, B, “Types of Renewable Energy. Hybrid Energy Systems”, 2017, pp 105-133

[5] renewable-energy-sources-infographic-vector-id502072950 (416×416)

[6] A. Azizi, “Modélisation optimisation d’un système de production d’énergie photovoltaïque avec un système de stockage hybride ”, Thèse de doctorat, Université Badji Mokhtar -Annaba, 2019, pp

[7] a photovoltaique solar system - Search Images

[8] https://energytheory.com/solar-panel-components/

[9] connection of solar panels in series parallel - Recherche Images

[10] D. Tan and A. K. Seng. “Handbook for Solar Photovoltaic (PV) Systems”, Singapore

[11] B. Mohand Ali et B. Mohammed, ”Optimisation des performances d’un panneau solaire à air- Système Hybride PV/T (Etude expérimental)”, Thèse de mastère, Département de physique. Université de M’sila, 2022, pp

[12] solar-parabolic-dish-concentrator-1529663888-4008005.jpeg (433×333)

[13] parabolic solar collectors - Recherche

[14] J. Zanis, “Classification of solar collectors”, Latvia University of Agriculture, Faculty of Engineering, 2008, pp

[15] R. I. Saeed. and A. K. Ibrahim, “A Review of Recent solar collectors: Classifications, Development, Applications and New Systems”. IRJMETS, Volume 04, University of Mosul, Iraq, 2022

[16] thermal solar collectors - Recherche Images

[17] S. Altınkök, A. Altınkök, "Photovoltaic Thermal PV/T Solar Panels and Practical Applications". The Black Sea Journal of Sciences, 14, 2, 2024, pp 683-699.

[18] A. K. Tiwari, K. Chatterjee, S. Agrawal, G. K. Singh, "A comprehensive review of photovoltaic-thermal (PVT) technology: Performance evaluation and contemporary development". Energy Reports, 10, 2023, pp 2655-2679.

[19] WGJ Helden, RJC Zolingen, HA Zondag. "PV thermal systems: PV panels supplying renewable electricity and heat". Progr Photovoltaics: Res Appl 2004;12: 415–26.

[20] Wolf, M., "Performance analyses of combined heating and photovoltaic power systems for residences", Energy Conversion, 16, 1976, pp. 79-90.

[21] L. H. Florschuetz, "Extension of the Hottel-Whiller bliss model to the analysis of combined Photovoltaic/Thermal flat plate collectors". ICSE Solar Energy Society Meeting, Winnipeg, Canada, 15-20 August 1979.

[22] C. H. Cox, and P. Raghuraman, "Design considerations for flat - plate-photovoltaic/thermal collectors". Solar Energy, 35, 1985, pp. 227-241.

[23] A. K. Bhargava, H. P. Garg and R. K. Agarwal, "Study of a hybrid solar system-solar air heater combined with solar cells", Energy Conversion and Management, 31, 5, pp 471-479.

[24] J. Prakash. "Transient analysis of a photovoltaic-thermal solar collector for co-generation of electricity and hot air/water". Energy Convers. Mgmt, 35, II, 1994, pp 967-972.

[25] B. Sandnes, J. Rekstad, "A photovoltaic/thermic (PVT) collector with a polymer absorber plate: experimental study and analytic model", Sol Energy, 72, 2002, pp 63-73.

[26] K. Sopian, H.T. Liu, K. S. Yigit, S. Kakac, and T. N. "Veziroglu, Performance analysis of photovoltaic thermal air heaters". Energy Convers. Mgmt, 37, 11, 1996, pp. 1657-1670.

[27] K. Nagano, T. Mochida, K. Shimakura, K. Murashita, S. Takeda, "Development of thermal photovoltaic hybrid exterior wallboards incorporating PV boards in and their winter performances", Solar Energy Materials and Solar Cells, 77, 2003 pp 265-282.

[28] J.K. Tonui, Y. Tripanagnostopoulos, "Improved PVT solar collectors with heat extraction by forced or natural air circulation", Renewable energy, 32, 2007, pp 623-637

[29] G. L. Jin, et al “Evaluation of Single-Pass Photovoltaic-Thermal Air Collector with Rectangle Tunnel Absorber”, Solar Energy Research Institute, University Kebangsaan Malaysia. 2010.

[30] M. Y. Othman, F. Hussain, K. Sopian, B. Yatim, H. Ruslan, “Performance study of air-based photovoltaic-thermal (PV/T) collector with different designs of heat exchanger”. Sains Malaysiana, 42, 2013, pp 1319–1325

[31] M.E.A. Slimani, M. Amirat, I. Kurucz, S. Bahria, A. Hamidat, W.B. Chaouch, 2017. “A detailed thermal-electrical model of three photovoltaic/thermal (PV/T) hybrid air collectors and photovoltaic (PV) module: Comparative study under Algiers climatic conditions”. Energy Convers. Manag. 133, pp 458–476.

[32] M. Hosseinzadeh, A. Salari, M. Sardarabadi, M. Passandideh-Fard, “Optimization and parametric analysis of a nanofluid based photovoltaic thermal system: 3D numerical model with experimental validation”, Energy Conversion and Management, 160, 2018, pp 93-108

[33] J. H. Lee, S. G. Hwang, G. H. Lee, “Efficiency Improvement of a Photovoltaic Thermal (PVT) System Using Nanofluids”, Energies, 12, 16, 2019

[34] S. Alsaqoor, A. Alqatamin, A. Alahmer, Z. Nan, Y. Al-Husban, H. Jouhara, “The impact of phase change material on photovoltaic thermal (PVT) systems: A numerical study”, International Journal of Thermofluids, 18, 2023

[35] S. Boulhidja, A. Bourouis, T.E. Boukelia, A. Omara, “Mixed convection air-cooled PV/T solar collector with integrated porous media”. Journal of the Brazilian Society of Mechanical Science and Engineering, 2024.

[36] M. A. V. Rad, A. Kasaeian, S. Mousavi, F. Rajaee, A. Kouravand, , “Empirical investigation of a photovoltaic-thermal system with phase change materials and aluminum shavings porous media”, Renewable Energy 167, 2021, pp 662-675

[37] https://en.wikipedia.org/wiki/Polypropylene

[38] M. S. M. Saleh, “Numerical Study of mixed convection in eclosures during the flow of a nanofluid”, Doctoral Degree Thesis, Ibn Khaldun University of Tiaret, 2023

[39] Hooman. K, “A perturbation solution for forced convection in a porous saturated duct”. J Comput Appl Math 211, 2008, 57–66

[40] A. Radwan, M. Ahmed and S. Ookawara "performance enhancement of concentrated photovoltaic systems using a microchannel heat sink with nanofluid", Energy Conversion and Management, Vol. 119, pp. 289-303. 2016.

[41] https://th.bing.com/th/id/OIP.WK75NxwqcxY-YNQGMpnDVQHaFQ?rs=1&pid=ImgDetMain

Abstract

This study optimizes photovoltaic thermal (PVT) collector performance through a reduced flow passage section by the integration of a solid layer beneath the last collector's cells. Numerical simulations, employing the Finite Volume Method and SIMPLE Algorithm, compared a conventional PVT collector with the modified design under varying solid layer dimensions. Results showed a significant 17.86% increase in thermal efficiency with increasing Re (500-1500) in the conventional design, while electrical efficiency peaks at the beginning and end of the day and reaches its lowest point during the afternoon. The modified design exhibited substantial performance gains, achieving up to 3.17% and 9.33% improvements in electrical and thermal efficiencies, respectively. Under identical Re and solar radiation conditions, the modified design significantly outperformed the conventional design, demonstrating 9.74% and 19.23% enhancements in electrical and thermal efficiencies. This passive design modification, incorporating a solid layer to reduce flow passage section, thus presents a highly effective method for enhancing PVT collector performance.

Keywords: PVT collector, Solid layer, FVM, Forced convection.